JULY 2018

M.Sc in Engineering Physics

GÖKHAN BİRLİK

UNIVERSITY OF GAZIANTEP

GRADUATE SCHOOL OF

NATURAL &APPLIED SCIENCES

SYNTHESIS AND THERMOLUMINESCENCE PROPERTIES OF Eu DOPED $CaMoO_4$

M.SC THESIS

IN

ENGINEERING PHYSICS

BY

GÖKHAN BİRLİK

JULY 2018

Synthesis and thermoluminescence properties of Eu doped $CaMoO_4$

Master Thesis

in

Engineering Physics

University of Gaziantep

Supervisor

Assoc.Prof.Dr. Vural Emir KAFADAR

by

Gökhan BİRLİK

July 2018

REPUBLIC OF TURKEY
GAZIANTEP UNIVERSITY
GRADUATE SCHOOL OF
NATURAL AND APPLIED SCIENCES
ENGINEERING PHYSICS

Name of Thesis: Synthesis and Thermoluminescence Properties of Eu Doped $CaMoO_4$

Name of the student: Gökhan Birlik

Exam date: 06.07.2018

Approval of Graduate School of Natural and Applied Sciences.

Prof.Dr.A. Necmeddin YAZICI
Director

I certify that this thesis satisfies all the requirements as a thesis for the degree of Master of Science.

Prof. Dr. Ramazan KOÇ
Head of Departmant

This is to certify that we have read this thesis and in our consensus opinion, it is fully adequate, in scope and quality, as a thesis for the degree of Master of Science.

Assoc. Prof. Dr. V. Emir KAFADAR
Supervisor

Examine Committee Members:	Signature
Assoc.Prof.Dr.V. Emir KAFADAR	.....
Assoc.Prof.Dr. Hüseyin TOKTAMIŞ	.....
Assist.Prof.Dr. Necmettin NUR	.....

I here declare that all information all information in this document has been obtained and presented in accordance with academic rules and ethical conduct. I also declere that as required by these rules and conduct, I have fully cited and referenced all material and results that are not original to this work.

Gökhan BİRLİK

ABSTRACT

SYNTHESIS AND THERMOLUMINESCENCE PROPERTIES OF Eu DOPED $CaMoO_4$

BİRLİK, Gökhan
M.Sc. in Physics Engineering
Supervisor: Assoc.Prof.Dr. Vural Emir KAFADAR

July 2018, 49 pages

Rare-earth ion doped calcium molybdate ($CaMoO_4$) has attracted much interest due to its wide luminescence applications. These include optical filters, solid state lasers, LED (light emitting diodes), scintillators, microwave dielectrics, cryogenic detectors and fluorescent lamps. Moreover, some of its attractive features include a high melting point (1445–1480 ^oC), refractive index (1.98), effective average decay time (14 μs), photo electron yield (9%) and it is also chemically resistant and non-hygroscopic. $CaMoO_4$ shows a broad blue and/or green luminescence emission peak in the range 350–650 nm with a peak maximum around 500 nm. In the given study Eu doped Calcium Molybdate phosphors have been sythesized using the complex polymerization method (cpm) and the thermoluminescence properties were investigated in detail. Computerized glow deconvolution (CGCD) method was used to determine the kinetic parameters namely the order of kinetics (*b*), activation energy (E_a) and the frequency factor (*s*) associated with the dosimetric thermoluminescent (TL) glow peaks of $CaMoO_4$: Eu after different dose levels with β irradiation.

Keywords: Thermoluminescence, $CaMoO_4$: Eu, kinetic parameters

ÖZET

EVROPYUM KATKILI $CaMoO_4$'ün SENTEZLENMESİ VE TERMOLÜMİNESANS ÖZELLİKLERİ

BİRLİK, Gökhan
Yüksek Lisans Tezi, Fizik Mühendisliği
Danışmanı: Doç.Dr. Vural Emir KAFADAR

Temmuz 2018, 49 sayfa

Nadir toprak iyonu katkılı kalsiyum molibdat ($CaMoO_4$) geniş lüminesans uygulamaları nedeniyle çok ilgi çekmiştir. Bunlar arasında optik filtreler, katı hal lazerleri, LED (ışık yayan diyotlar), sintilatörler, mikrodalga dielektrikler, kriyojenik dedektörler ve flüoresan lambalar bulunur. Ayrıca, çekici özelliklerinden bazıları, yüksek erime noktası (1445-1480 ^oC), kırılma indeksi (1.98), efektif ortalama bozunma süresi (14 μs), foto elektron verimi (%9) ve kimyasal olarak dirençli ve nem çekmemesidir. $CaMoO_4$, 350-650 nm aralığında maksimum 500 nm'lik bir pik ile geniş bir mavi ve / veya yeşil parlaklık emisyon tepesi gösterir. Yapılan çalışmada, Eu katkılı Kalsiyum Molibdat fosforları karmaşık polimerizasyon yöntemi kullanılarak sentezlenmiş ve termolüminesans özellikleri detaylı olarak araştırılmıştır. $CaMoO_4$: Eu'nin β ışınlaması sonrası kinetik parametre değerleri; kinetik derece (b), aktivasyon enerjisi (Ea) ve frekans faktörünün (s) belirlenmesi için bilgisayarlı ışıma eğrisi analizi (CGCD) metodu kullanılmıştır.

Anahtar Kelimeler: Termolüminesans, $CaMoO_4$: Eu

To my family…

ACKNOWLEDGEMENTS

I would first like to thank my thesis advisor the number Assoc.Prof.Dr. Vural Emir KAFADAR of the faculty member at Gaziantep University. He has set an example of excellence as a researcher, mentor, instructor, and role model. I am also very grateful for guiding and supporting me over the years.

I warmly thank Assoc. Prof. Dr. Fatih Mehmet Emen from Mehmet Akif Ersoy University for the synthesis of the sample.

I would especially like to thank my family for love, support, and encouragement.

TABLE OF CONTENTS

LIST OF TABLES

LIST OF FIGURES

LIST OF SYMBOLS

A_h : Recombination transition coefficient for electrons in the conduction band with holes in centers

A_n : Transition coefficient for electrons in the conduction band becoming trapped (volume/until time m^3sec^{-1})

A_m : Transition coefficient for holes in the valance band becoming trapped in the hole centers

b : Kinetic order

β : Heating rate

CGCD : Computer Glow Curve Deconvolution

E or E_a : Activation energy (trap depth)

E_c : Bottom of the conduction band

E_f : Energy Fermi level

E_g : Band gap

E_v : Top of the valance band

ET : Electron Traps

FOM : Figure of Merit

HT : Hole Traps

I : Thermoluminescence intensity

I_m : Peak intensity

k : Boltzman's Constant

N : Concentration of available electron trapsin the crystal (in m^{-3})

n : Concentration of the filled electron traps in the crystal (in m^{-3})

n_o : Number of trapped electrons at the initial time $t_0 = 0$

n_c : Concentration of electrons in the conduction band (per unit volume m^{-3})

N_h : Concentration of available hole centers

n_h : Concentration of holes in the recombination centers

n_v : Concentration of holes in the valance band

m : Concentration of holes trapped at R (m^{-3})

p : Probability per unit time of release of an electron from the trap

R : Recombination centers

s : frequency factor

T : Temperature

T_m : Peak temperature

TL : Termoluminescence

TLD : Thermoluminescence Dosimetry

CHAPTER 1

INTRODUCTION

1.1 What is thermoluminescence

The substances like insulators or semiconductors absorb energy while irradiated at a given temperature. If the substances are heated w emay observe a light emission which can be called as luminescence or thermoluminescence. Over 200 ^{o}C or at high temperatures a substance may also emit infra-red radiation. This process is called black body radiation. The thermoluminescence is to be produced if the sample is exposed to ionising radiation. So that, electrons with high energy are trapped within the sample, and the phenomena of the thermoluminescence (TL) can be noted in semiconductors and insulators which features the electrons in defect positions in the stability circumstance. The light must be emitted when these trapped electrons out of the trap and come down to the lower energy level through the potential barrier by heating the material [1].

Thermoluminescence (TL) is a misnomer in the conventional sense of the names of luminescence processes like Cathodoluminescence, Chemiluminescence, Electro-luminescence and Bioluminescence. The excitation is achieved by any type of ionizing radiation. It is also necessary to distinguish clearly between thermoluminescence and incandescence emissions from a material being heated: the luminescence usually lies in a spectral region where the material is non-absorbing; the incandescence emissivity is strongest where absorptivity of the material is the maximum. There is also a wide gap between the temperatures of occurrences of these two emissions, incandescence occurring at very high temperatures near the melting point of the respective material. The highest temperature at which TL has been reported for any solid is around 650°C. Normally it is understood that no TL can be observed at temperatures far lower than the excitation temperature, there are however

exceptions and these are distinguished as cryo-luminescence and cooling-down luminescence.It is heartening to note that in recent times the phenomenon of TL is being correctly referred as Thermally stimulated luminescence (TSL). The phenomenon of TL is usually qualitatively explained by using the band structure of the solids. The forbidden band gap can be imagined to contain some acceptor/donor metastable levels which are basically responsible for the observed TL [2].

The thermoluminescence (TL) phenomena could be observed at insulator and high band gap semiconductor materials. Because, the material should have necessary a band gap to observe TL phenomena. In the TL processes, the free charge carrieers in the conduction band (CB) after ionizing radiations become trapped at fault sites in a metastable situation within the band gap of TL materials. The trapped charges can then be released by heat stimulation and they pass the potential barrier to the CB and then will move to lower energy states which is called as luminescent or recombination center with the diffusion of light. This process is called as thermoluminescence (TL) [1]. Simply, in the TL phenomena, the material shoulde be firstly exposed to radiation at moderate temperatures such as room temperatures by the ionizing radition and then the material is heated at a a temperature range in which all the electrical charges that were trapped in charge traps which is called as metastable states have been thermally excited out from these traps grades until a temperature level and the luminescence entirely vanish. If one plotted the emission of light intensity versus temperature the evaluated curve is named as the thermoluminescent glow curve (GC) [2]. There are three basic components necessary for the production of TL. First, these materials must have a luminescence properties in order to produce (TL) like semiconductors and an insulators, but metals don't have this property. Second, the materials absorbing energy at some time when the ionizing radiation falls on them. Third, the light is coming out of the materials (luminescence emission) when heating these materials [2]. The thermoluminescence (TL) material absorbs (stored) some energy during exposure to ionizing radiation, and when heating this material will release the energy which is absorbed as a visible light. The major attributes required to make a good material thermoluminescence (TLD dosimeter) nominees are; the broad separator in which the intensity of the luminescence is linearly proportional to the absorbed dose. In most of the substances,

the super linearity and saturation (decay) for the intensity of the thermoluminescence at large doses is limits the linear interval. And the linear dose dependence determined the benefit range [3].

- Low dependence of the TL response to the type of radiation. If required, it can rely on the energy partially offset metal filters.
- High sense, i.e. the high thermoluminescence signals per unit these doses which are absorbed. And it is important to use this high sensitivity in medical dosimetric and personal, and also in environmental radiation monitoring.
- Low fading, it means that the capability to store absorbed dose longtime.
- Incomplex glow curve structure.
- The spectrum of the luminescence must be proportional with the ultimate spectral sensitivity of the photomultiplier.
- TLD sunstance must be chemically inactive, strong and radiation unyielding.

Thermoluminescence (TL) is the light emitted from thermal stimulation process after absorbing energy from the previous radiation. A curve is obtained (glow curve) during the readout by using a linear time-temperature heating profile after detection a thermoluminescence emission and plotting with respect to time. This evalutaed graph can be analyzed by introducing the parameter which is called the (order of kinetics) from an experimental method. The trapped electrons have two types of opportunities to jump to the down after they are jumping up by thermal energy to the conduction band. First is the process of the re-trapping or return to the same type of traps and second, is electrons recombine with holes accompanied by emission of the thermoluminescence light. When neglects the probability of the re-trapping process, therefore, the peak shape of the glow curve will be narrow because of the fast recombination process which is interpreted by Randall and Wilkins [4]. And the wide peak of the curve has interpreted by Garlick and Gibson when the re-trapping dominates and the recombination electrons with holes are suppressed [5]. The two explanations which are described above are termed the first and second order kinetics. The general order kinetics are entered between them to provide a continuance from separate two kinds of kinetics interpreted by May and Partridge [6].

The characteristics of the dosimetric for thermoluminescence materials rely mainly on the tarpping parameters which are responsible quantitatively the trapping-emitting centers and thermoluminescence issue. To determine the trapping parameters and so active region of study and different methods placed to derive the parameters of the glow curve. The TL curves from different various quartz samples are recorded by David and colleagues and affirmed that it was hard to compare thermoluminescence (TL) which were published from the various samples due to controversies in pre-irradiation treatment, heating rates, way of manufacture, and content of impurities, etc. [7]. Therefore, here the objective is to identify the trap parameters, TL sensisivity and the stability of thermoluminescence (TL) glow-peaks of the ($CaMoO_4$: D_y) specimens.

There are different prodeduress to calculate the trap parameters of the TL curves. To understand the behaviour, the peak should be isolated from the complex structure using some empirical ways. Shape of peak (PS) and Heating Rate (HR) ways are appropriate in determining the kinetic parameters. $CaMoO_4$:Eu has several overlapped peaks as in most thermoluminescence materials. There are basically two ways to get these parameters when glow curve contains more than one glow peak. First, each individual thermoluminescence (TL) peak insulated from other peaks by using the partial thermal annealing treatment. Second, computer based glow curve analysis may be used such as deconvolution [13]. There are a few difficulties in the use of the first method without any lose in the intensity while dealing with the interested peak. The main attractive property is not using any thermal treatment in the computer based deconvolution while determining the trap parameters of each peak. The disadvantage in the deconvolution way over classical ways comes from especially if the glow curve has a complex structure[1].

1.1.1 Luminescence

The material can be absorbed and re-emitting some of its energy in the light of a longer wavelength when the radiation falling on it (Stoke's law) and this process is called luminescence. Luminescent material can be characterized from the wavelength of the light emitted but it is cannot be characterized from the incident radiation. Usually the phenomenon of luminescence in most studies is attached with the emission of the visible light but other wavelengths like (ultra-violet or infra-red) may

be emitted [2]. After absorbing radiation the emission of the light takes place a characteristic time (τ_c) and this parameter (τ_c) allows us to subdivide the process of luminescence as illustrated in the figure 1.1 The (τ_c) of fluorescence is smaller than (10^{-8}s) and (τ_c) of phosphorescence is greater than (10^{-8}s) by this difference we can distinguish between the phosphorescence and fluorescence.

Fluorescence emission is basically a spontaneous process because its (τ_c) value is smaller than (10^{-8}s), and happens simultaneously during absorbing the radiation and immediately ceases when the radiation ceases. Phosphorescence emission is the time interval which is starting the radiation absorption till reach to maximum intensity (t_{max}) and the (τ_c) value of the phosphorescence is greater than (10^{-8} s) and has been seen to continue for some time after removing the excitation. However, it is more complex to distinguish between phosphorescence and fluorescence when the time of delay is too short. And the phosphorescence itself can be subdivided into two main kinds [2]. One is the short period phosphorescence (τ_c <10^{-4}s) and another one is the long period phosphorescence (τ_c>10^{-4}s). The only thing to identify between the phosphorescence and fluorescence is the understand the temperature effect on the luminescence decay clearly through practical viewpoint. Phosphorescence is heavily dependent on temperature, whereas the fluorescence is not dependent on temperature [2].

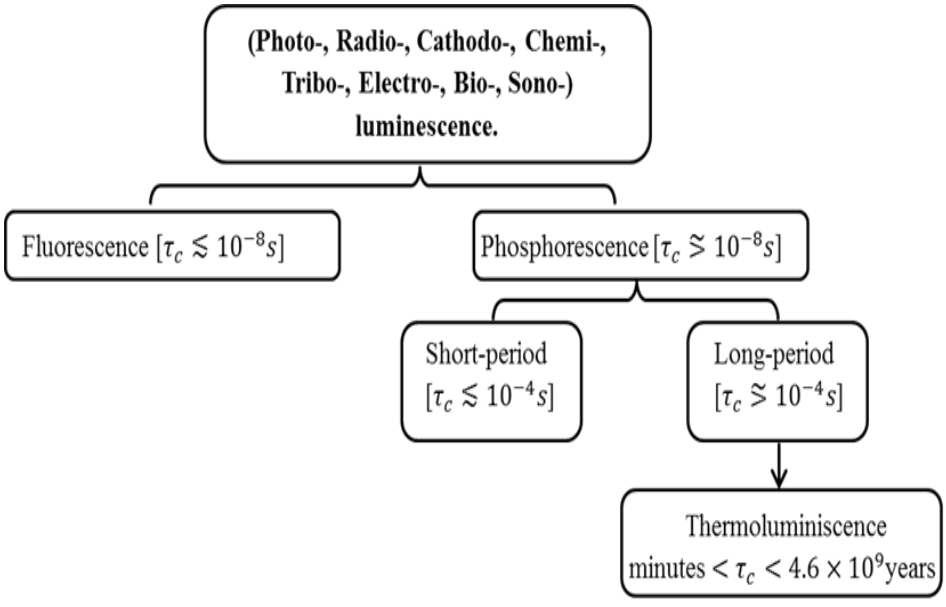

Figure 1.1 The "family tree" of the phenomenon of luminescence, the different between fluorescence and phosphorescence is due to the delay (τ_c) between emission and excitation [2].

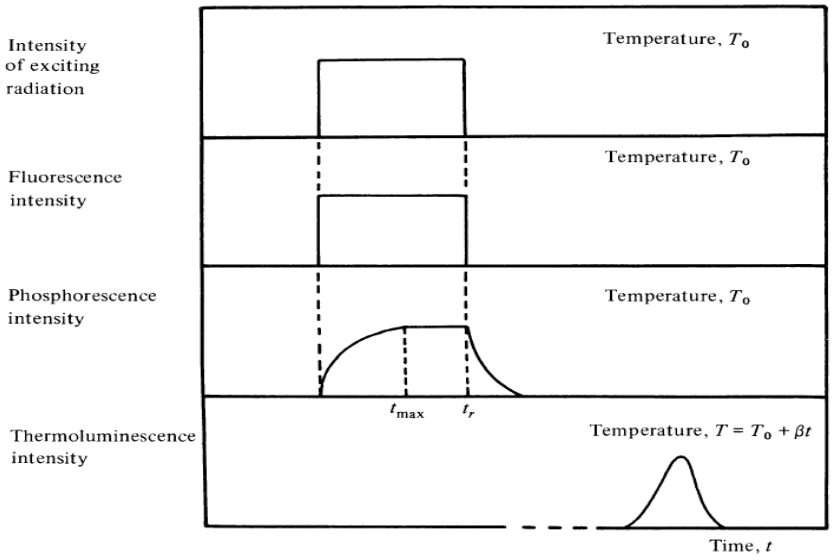

Figure 1.2 The relationship between absorption of radiation and the emission of phosphorescence, fluorescence and thermoluminescence. (T_0) is the temperature at which irradiation happens; (β) is the heating rate, (t_r) is the time of starting the decay of phosphorescence after ending irradiation time [2].

It can also be explained the luminescence emission by the energy transfer to the electrons of the material, (transition (i) in figure 1.3a) means agitating the electron from the ground level (g) to the excited level (e), and when this agitated electrons come down to its ground state emits luminescence photon (transition (ii)). Thus, for fluorescence the delay between transition (i) and (ii) is ($<10^{-8}$). And this process is independent of temperature.

Chen[8] has presented the first interpretation of temperature dependent phosphorescence. In the figure (1.3b) the energy level figure is changed with a metastable state (m) in the forbidden gap between the excited state (e) and the ground state (g). When an electron excited from the ground state (g) to an excited state (e) may be trapped in (m) then stay in there till if one given necessary energy (E) to turn to the excited state (e) and is subject to a natural progress back to the ground level (g), with subsequent emission of light. Thus the delay observed in phosphorescence complies with the time which is spends the electrons in the trap (m).

From the arguments of thermodynamic it may demonstrate that the life time (τ) at which the electron stays in the trap at T can be found as:

$$\tau = s^{-1}\exp = (\frac{-E}{kT}) \quad (1.1)$$

s: the frequency factor, E: the the trap depth, k: the Boltzmann's constant. Thus that process depends exponentially on temperature [2].

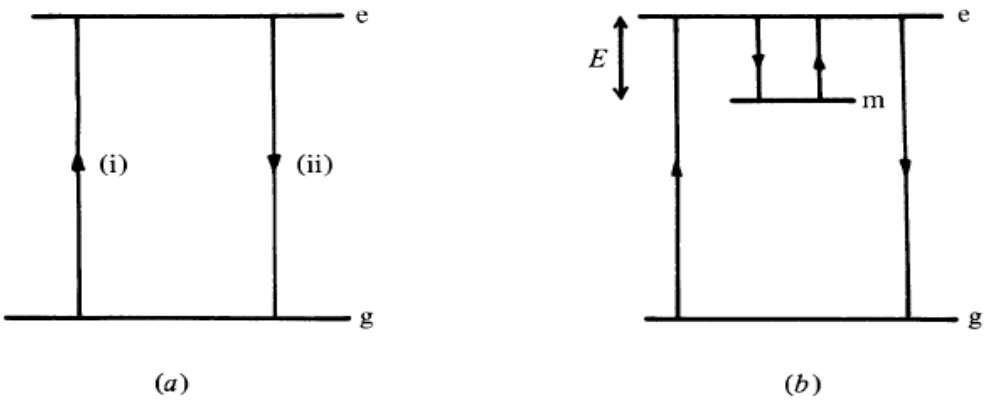

Figure 1.3 The energy transitions in fluorescence process [2].

1.2 Requirements of a suitable TL material

A thermoluminescence (TL) phosphor which is used to measure the dose and it should combine the several properties, as a consequence, only reduce the choice to few inorganic compounds. A (TLD) phosphor has some properties which are more desirable and these properties are [8]: First, high concentration of the electron or hole traps and an efficient of light emission is needed. Second, Adequate store stabilization of the (electron) trap or (hole) trap to not cause any unwanted fading even during long storage of the ambient temperatures or a slightly increasing temperature (desert or tropical climates) or, the studies of the implantation of biomedical, temperature of the body. And this must be applied to the opposite end of the climate inside (the Arctic Circle) where the temperatures are low. Third, when the detector system (photomultiplier and filter combination) is responding well. The spectrum of the emission of the thermoluminescence (TL) light has least possibilities interfere with incandescence (infrared) emission of the hot phosphor and its surroundings areas. Forth, the distribution of the trap which does not complicate the procedure of evaluation because of the existence additional fading (low temperature or high temperature) peaks (that is maybe hard to anneal) and due to the process of

the re-trapping, etc. And must be completely annealing the phosphor during the procedure of readout, without changes its sensitivity and reading of the background or (linearity). The fifth, The temperature of the main peak (Tm) located between (180 ^{0}C and (250 ^{o}C). Increasingly, at the higher temperature the infrared emission from the hot model and the model holder interferes with the low dose measurement. The spectrum wavelength between about (300 nm) and (500 nm) are the most desirable only if sensitive system used specifically for UV. Sixth, the resistance against the environmental troublesome potential factors likes (humidity, gases, light, common fumes and organic solvent). If this is not possible, sealed the detector into a bulb of glass permanently. Seventh, the phosphor must be cheaper and easier for working with "one-way" dosimeter, and it must be non-toxic and does not deteriorate during storage for a long time. It is possible to use a small model only, taking into account if there are no spurious effects like (Tribo- or chemiluminescence, oxygen effects, etc.) and may be useful if can be prepared the material easily with the properties of reproducible in a naturally equipped laboratory of chemical. Eighth, for most applications, the desirable features, the low photon energy dependence of response in the extending range are depending on the particular use, a (high) or (low) thermal neutron sensitivity or a specific (LET) response can be the desirable properties.

1.3 Advantages of TL phosphors in personal dosimetry

The several advantages are found in (TL) systems for personal dosimetry [8]:

1) TL detectors are abundant in the form of powder or solid in a broad range of volume.
2) Practically, the thermoluminescence (TL) materials are not dependent on the rate of dose and on the angle of radiation incidence.
3) Thermoluminescence detectors are appropriate for postal service.
4) That it is possible to have a re-evaluation of the absorbed dose of irradiation of UV and readings of a high temperature peak (PTTL).
5) The minimum of detection is about (0.2) mGy;
6) Some materials (TL) have a near tissue -equivalent configuration (LiF, $Li_2B_4O_7$, MgB_4O_7, BeO) which cancels the need to get energy debugging;
7) A large monitoring services are evaluated from automated /computerized.

1.4 General features of thermoluminescence

Luminescence of many solid materials is unlisted in the category of either (Luminescence) or (Thermoluminescence), but represents a various phenomenon when rises their temperature to incandescence. Luminescence in solids can be occurred mainly by (ultra-violet radiation, γ or X radiation, energetic electrons, nucleons and pions, and as well as from an electric field). And also can shine solids by some of the chemical and biological processes. Emissions largely depends on the distinctive attributes of impurity atom, which works as an activator. When the exciting radiation stopped, some of the materials have the ability to emit light in the range of (visible) or (near visible) this phenomena is called luminescence. A period of continuation of this afterglow can be too short is about (10^{-8} to 10^{-7}s). But in many instances there may be an extra element of the afterglow which continued for much longer. This element is called phosphorescence, typically established from the role attributed to metastable states of activator in the host material [8].

1.5 Defects and color centers

The centers of the defects and color are axis of any process of luminescence, and it is appropriate to provide these concepts here in an elementary method [18]. The point defects are between these simple defects that are found in the structure of the crystal and which are easily able to mathematically formulate. Creation states inside the energy gap of the host material because there are the defects and impurities within them and these states may be the type of (an electron and hole). And these states which are created have the ability for light absorption from some spectrum of the visible part. The crystal is colored and, thus, described these states also as the (color centres). The names of different phenomena of the luminescence are given, as illustrated in the table 1.1 which reflects the kind of radiation that are used for emission excitation. The lists which are described in the below table are (the phenomena of luminescence and excitation method) [9].

1.6 Thermoluminescence Applications

The significant development has been acquired in the thermoluminescence application for practical usage during the past twenty years or so. And the application which is developed very widely, however its usage in radiation measurements are

very wide such as health physics, biomedical science, radiation protection and control. At the same time notable development in the TL technique found a place in its applications in dating of archaeological and geological [10-11]. The recent thermoluminescence application is related to the date of the sand dunes, which have the effects in their movement study and some of the other sides of the desert environment. Interesting, but it is not developed sufficiently, the applications which have been mentioned in the science of forensic which means the characterization of suspicious materials and determine the forged objects which are susceptible for thermoluminescence (TL) investigations. İn industry (study of burnt concrete of fire – damaged buildings and of industrial pollutants) and, via the TSC mechanism, in solid state ionography [12].

Table 1.1 The phenomena of luminescence and excitation method [1].

Luminescence Type	Excitation Type
Bioluminescence	Biochemical reactions
Cathodoluminescence	Electron beam
Chemiluminescence	Chemical reactions
Electroluminescence	Application of an electric field
Photoluminescence	U. V. and infrared light
Piezoluminescence	Pressure (10 tons m^{-2})
Triboluminescence	Mechanical /Frictional forces
Radioluminescence	Ionizing radiation
Sonoluminescence	Sound waves
Fluorescence Phosphorescence light Thermoluminescence Lyoluminescence	Ionizing radiation, U.V. and visible

CHAPTER 2

THEORY OF THERMOLUMINESCENCE

2.1 Basic concepts of thermoluminescence (TL) in solids

Daniel et al [13] was the first person who used the applications of the thermoluminescence (TL) phenomenon for the purposes of dosimetry. In spite of that phenomena of TL have been known for a long time in order to develop new thermoluminescence materials, it has been implemented a lot of researches to understand and improve the characteristics of the materials. In these days, a TLD is the dosimetric technique which is established well with applications in the domains like (personnel, environmental and clinical dosimetry). Thermoluminescence dosimetry (TLD) is based on that material which emits light while they are heated, after exposure these materials, to ionizing radiation. The energy levels which are existing among the forbidden energy band gap, due to the impurities existence in the thermoluminescence materials and these are the crucial reason for the process of thermoluminescence. And as a way of detecting that the thermoluminescence (TL) sensitivity is unparalleled, during presence these defect levels. Townsend and Kelly [7]. Appreciate that the technology is able to detect at least (10^9) levels of defects in the model. In order to put this number in the proper perspective, the important thing that should be realized that the purity of the model is (6) orders of high magnitude. On the one hand, the high sensitivity allowed to identify a very low radiation dose, but it handicaps us to investigate the relation between the defects involved in this process and luminescence in the other hand. And for the various types of dosimeter the sensitivity of thermoluminescent material will be various. A process of relaxation of emitting light during the thermal stimulation is thermoluminescence. The traps are generated in (dosimetric) by high energy radiation. Appears on the thermoluminescence (TL) curve a series of peaks, and these attributable to trap levels which is featured by a different activation energies.

The theoretical description of the thermoluminescence (TL) usually assumes Standard traps spatial distribution and centers of recombination [1]. The thermoluminescent dosimetry has been studied by many investigators during the past ten years [14-15] .When the matter absorbs ionizing radiation, and eventually most of these energy which is absorbed goes into heat, and the chemical bonds are broken just by dissipation a small part of this energy. So small part of the energy in some materials are stored in metastable energy states such as (phosphorus). If the material is heated, and later can be restored some of this energy as visible photons. The releasing of the visible photons by thermal means is the luminescence (TL) [16-17]. Some of the phosphors have very good dosimetric characteristics and now widely used for radiation monitoring and dosimetry. In the thermoluminescent dosimetry, the effects upon the glow curve of thermal annealing are quite important.

The below figure (2.1) explains the phenomena of thermal excitation of luminescence which is said that when a thermoluminescence material absorbs some of that energy which is stored during the period of exposure this material to ionizing radiation. When it is heated, released this energy which is stored as a visible light. In fact that the thermal excitation does not represent thermoluminescence (TL), but TL refers to the luminescence stimulation in a model that is thrilled in a various method. In order to produce or (emit) light again from thermoluminescence material must be reheating this material and re-exposed to the ionizing radiation. The capacity of the storage energy of a thermoluminescence substance can be used as dosimetric measurements [18].

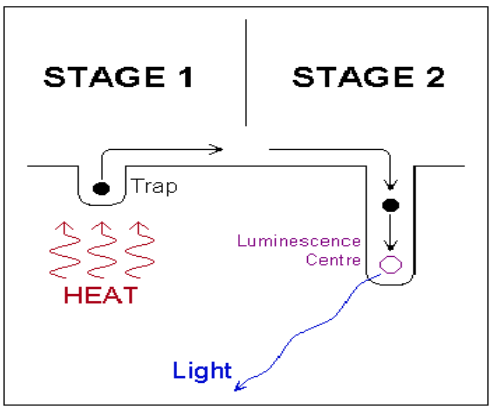

Figure 2.1 The phenomena of thermal excitation of luminescence [8].

2.2 The OTOR (One Trap One Centre Model)

The theory of energy band for solid materials interprets the properties of the observed thermoluminescence (TL). Most electrons are residing in the valence band in an ideal (semiconductor or insulator) crystalline. Conduction band is the second highest band, which can be occupied by electrons, and the other band which has existed between these two bands is the forbidden band gap. And (E_g) is the difference of energy between the (V.B) and the (C.B). However, whenever there are impurities inside the lattice, or if there are structural defects happens in a crystal, in this state the electrons have the possibility of having energies that are prohibited in an ideal sample. In this model ther are two levels, one is located at the bottom of (C.B) and the other is located on the upper part of (V.B) as illustrated in figure (2.2). The potential of the trap of the electron is (T) and it is located on the highest level and over the (E_f) and it is hollow in the state of equilibrium; before the radiation exposure and the (electrons and holes) generation. The potential hole trap (R) is the other level that can operate as a (center of recombination) [6].

The energy absorption ($h\gamma > Eg$) is result of ionizing the valence electrons, and produces the electron and holes pairs. After the process of heating there will be produced free charge carriers in the valence band (VB) conduction band (CB). This is a transition (a) in the below figure. This process is resulted with the recombination of the e-h pairs or re-trapping. In this case an amount of energy is to be freed because of direct recombination that might raise luminescent center [6].

Under the light emission, the center of luminescence relaxes, i.e, returns to the ground state. And with that, trapped a specific percentage of the charge carriers, in the materials (semiconductor and insulator). Trapped the holes in (R) and the electrons are trapped at (T) these are transition (b) as shows in the figure. The Arrhenius equation describes the probability per unit time (p) for releasing an electron from the trap:

$$p = s\, exp\{-E/kT\} \tag{2.1}$$

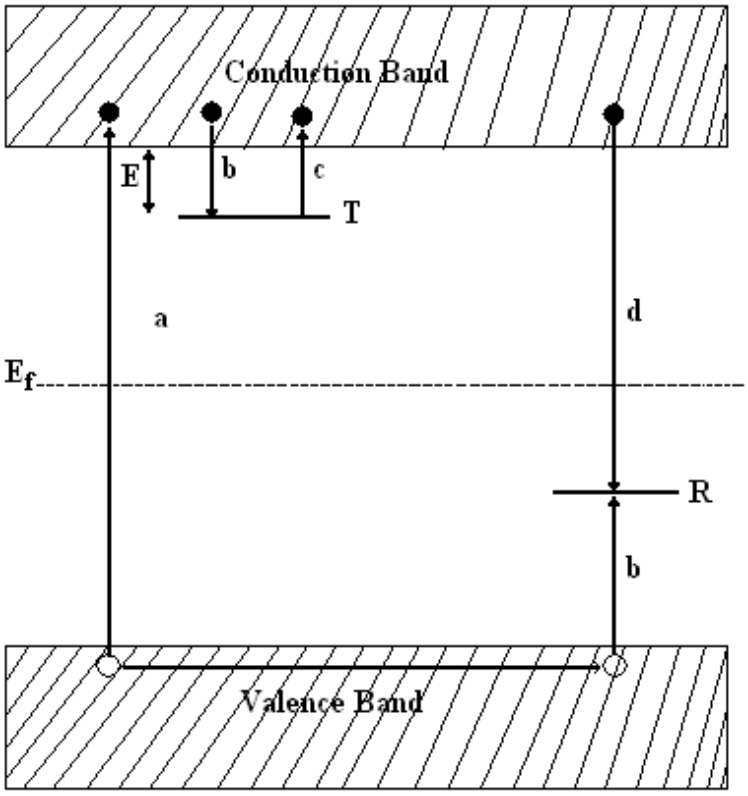

Figure 2.2 The electronic transitions in a thermoluminescence material using the energy band model [8].

The trapped electrons will stay in the trap for a long period if the trap depth is much bigger than (kT_0), where (T_0) is the irradiation temperature, until radiation exposure there will exist a lot of electrons population which are trapped, But must be exist at the level (R) an equal trapped holes population, due to the creation and annihilation the (electrons and holes) in pairs. So that in the equilibrium the Fermi level (E_f) is located above the state (R) and below the state (T). The reaction track is always open for returning to the state of the equilibrium, but because the equilibrium disturbance was performed during exposure to the ionizing radiation at low temperature in comparison with (E/k), and the rate of relaxation that is specified by the equation (2.1) is small. The stability may come back quickly with increasing the heat level of the thermoluminescence substances higher than (T_0). And by this the detrapping probability will increase and now the electrons going out (or freed) from the trap and move to the (C.B). Moves the electrons from the conduction band of the substance until recombine with the (holes) at the recombination center (R). This centre of recombination is a centre of luminescence in the simple model, where the e – h recombination go out from the centre to excited states, and come back to the ground

level after emitting light, i.e. (TL). And the thermoluminescence intensity I(t) in photons per second at any time (t) during the heating is commensurate with rate of holes and electron recombination at the centre of recombination (R). If the concentration of holes trapped at (R) is (m (m^{-3})), can be written the intensity of the thermoluminescence (TL) as the:

$$I(t) = -dm/dt \tag{2.2}$$

In here we suppose that a photon produces from all recombination and that are detected from each photon which were produced. The recombination rate is proportional to the number of free electrons (n_c) in the conduction band and the hole concentration (m).

$$I(t) = -dm/dt \; = \; n_c \, m \, A \tag{2.3a}$$

The constant A is the probability of recombination expressed in volume per unit time which is supposed to be not depent on the temperature. The change rate (*-dm/dt*) of the concentration of trapped electrons (n) is equal to the rate of the thermal release (*np*) minus the rate of the retrapping (n_c *(N-n)*A_r),

$$-dn/dt \; = np - n_c(N - n) \tag{2.3b}$$

where (*N*) are the electron traps concentration and (A_r) is re-trapping probability (m^3/s). Similarly average concentration of the free electrons (dn_c/dt) is equal to the thermal release rate (np) minus the re-trapping rate (n_c (N-n)A_r) and the recombination rate, (n_c m A).

$$dn_c/dt = np - n_c \, (N - n)A_r - n_c mA \tag{2.3c}$$

Equation (2.3a) and the equation (2.3c) described the traffic of the charge carrier during the process of releasing the trapped electron from the trap of a (single-electron) and the recombination in a (single-centre). The thermoluminescence (TL) produced by the holes release, the rate equations are same to the equation (2.3a). The basis of a lot of analyzes for the thermoluminescence (TL) phenomena are formed by these equations. A general analytical solution can not be done and these equations must be solved by some simplifying assumptions for developing an analytical expression. The assumption which is called by Chen and McKeever [8] is a quasi equilibrium assumption. And this is due to that the concentration of free electron is

quasi stationary in the conduction band, and this assumption at any time is an important assumption;

$$|dn_c/dt| \ll |dn/dt| \quad , \quad |dn_c/dt| \ll |dm/dt| \tag{2.4}$$

This assumption produces the trapped electrons and the trapped holes in pairs during the irradiation and charge neutrality dictates therefore,

$$n_c + n = m \tag{2.5}$$

and ($n_c \approx 0$) it means that ($n \approx m$) and,

$$I(t) = -\, dm/dt \;\approx\; -dn/dt \tag{2.6}$$

when (dn_c/dt) is approximately equal to zero, one can get from the equation (2.3a) and the equation(2.3b) is;

$$I(t) = (mAns \exp\{-E/kT\})/((N-n)A_r + mA) \tag{2.7}$$

2.2.1 First-order kinetics

Analytically, we can't solve the equation (2.7), but it can be solved by adding the additional simplifying assumption. The Randall and Wilkins [4] neglected the rate of retrapping ((N-n) Ar) from equation (2.7) during the heating stage. The transport of charges can be calculated from this differential equation is called First-order kinetics. The solution of equation (2.7) gives:

$$I(t) = -(dn/dt) = n_0 s\, exp\{-E/kT\}\exp\{-s\int_0^1 \exp\{-E/kT(t')\}dt'\} \tag{2.8}$$

In accordance with the below equation the temperature is increased as a linear function of time, and the total number of trapped electrons at a time (t = 0) is (n_0)

$$T(t) = T_0 \;+\; \beta t \tag{2.9}$$

where,

(β) is the heating rate and (T_0) is the temperature at the time (t = 0). Then, the intensity *I(t)* as a function of temperature becomes as;

$$I(t) = -\frac{1}{\beta}(dn/dt)\, n_0 \frac{s}{\beta} exp\{-E/kT\}\exp\{-\frac{s}{\beta}\int_{T_0}^{T} \exp\{-E/kT'\}dT'\} \tag{2.10}$$

The equation (2.10) is a famous Randall–Wilkins expression of the first-order for a peak of a single glow. The figure (2.3) explains the properties of the equation of the Randall–Wilkins. The difference of intensity *I(t)* can be observed in the figure (2.3a), if (n_0) varies from (n_0=0.25 m^{-3}) till (n_0=2 m^{-3}) while (E=1 eV, s=1.0×10^{12} s^{-1} and β=1 K/s) are remaining constant.

It can be pointed that the temperature remains constant at the maximum of the peak (Tm), and this is a feature of all thermoluminescence (TL) curves of the first-order. It can be found the condition for the maximum by placing $\left(\frac{dI}{dt}\right) = 0$ (or, it is simple from $\left(\frac{d\ ln\ I(T)}{dt} = 0\right)$ we can obtain the following equation.

$$(\beta E/kT_m^2) = s\ \exp\{-E/kT_m\} \tag{2.11}$$

The (n_0) disappeared from the equation (2.11) it means that (T_m) is independent of n_0. It can also be seen that each point of the curve is proportional to n_0. In dosimetric application the n_0 parameter is the most important one because it is proportional to the absorbed dose. Also it is easy to find out that the n_0 is equal to the area under the glow peak.

$$\int_0^\infty I(t)dt = -\int_0^\infty \frac{dn}{dt}\ dt = -\int_{n_0}^{n_\infty} dn = n_0 - n_\infty \tag{2.12}$$

When ($t\rightarrow\infty$) the (n_∞) is zero. In the figure (2.3(b)) the activation energy (*E)* changes from (0.8 eV) to (1.2 eV). As illustrated in the figure (2.3(b)), the peak reaches to high temperature when increases the value of the activation energy *E*, and this is leading to a decrease in height and increases the peak width, but the area does not change, it is mean that n_0 is constant.

It can be also observed the same changes but in the opposite direction as seen in the figure (2.3(c)). The peak reaches to low temperature when increases the value of (s), and this leads to increases the height of the peak and reduces the width of the peak. But the figure (2.3(d)) one can be seen that when the rate of heating is increased the peak is transferred to the high temperature side of the curve leading to a decrease in height and increases the peak width, specifically as in the case of diminishing (s).

This can be predicted when (s) and (β) shown as a ratio of (s/β) in the equation (2.10). And it is important for knowing the four parameters, the first two parameters

are the major physical parameters (E) and (s) which are named as the parameters of the trapping, and determined by the properties of the trapping center. The last two parameters could be determined experimentally by identifying or selecting a particular dose (n_0) and as well as through the reading of the signal at a particular rate of heating. The assessment in equation (2.11) can be approximated the integral by the series of asymptotic due to the fact that in the integration of the linear heating case is not elementary on the right side [6].

For many applications this is appropriate to describe the peak by using the trap parameters such as the maximum temperature (Tm) and the maximum peak intensity (I_m). Kitis et al [19] showed that the equation. (2.11) could be accurate approximated by:

$$I(T) = I_m \exp[1 + \frac{E}{kT}\frac{T-T_m}{T_m} - \frac{T^2}{T_m^2} \exp\left\{\frac{E}{kT}\frac{T-T_m}{T_m}\right\}(1-\Delta) - \Delta_m \,] \qquad (2.13)$$

Where ($\Delta = \frac{2kT}{E}$) and ($\Delta_m = \frac{2kT_m}{E}$) . Newly, Pagonis et al [30], have showed that the first-order (TL) curve is described accurately by Weibull distribution function and these expressions may be appropriate for the purposes of peak fitting.

2.2.2 Second-order kinetics

The possibility in which the retrapping dominates was considered by Garlick and Gibson [5]. It means that (mA<<(N-n) Ar). They suppose the situation in which the trap is not saturated, i.e. (N>>n) and (n=m). Then, the equation (2.6) becomes.

$$I(t) = -\frac{dn}{dt} = s\frac{A}{NA_r}\, n^2 \exp\{-\frac{E}{kT}\} \qquad (2.14)$$

From the equation (2.14), it is clear that the (dn/dt) is proportional to (n^2) and the reaction is a 2nd order, and by the additional assumption when the probability of recombination (A) is equal to the probability of retrapping (A_r), the integration of the equation (2.14) becomes,

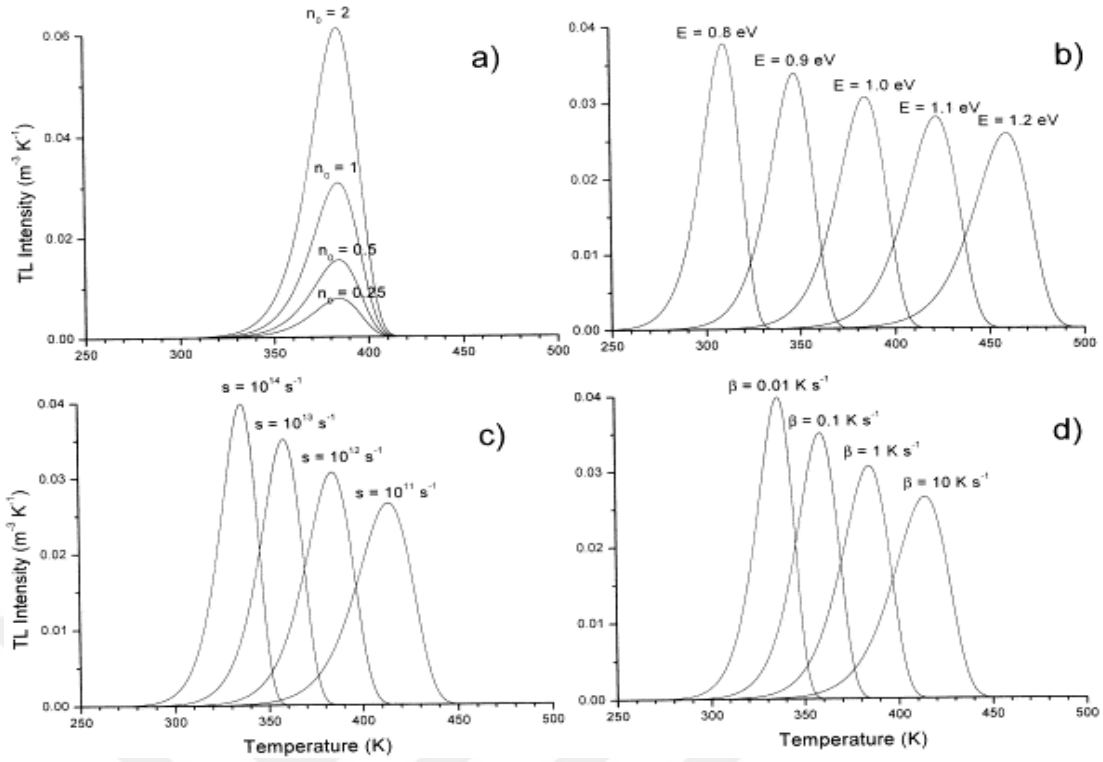

Figure 2.3 The properties of the Randall and Wilkins first-order thermoluminrscence (TL) equation, figure (a) explains the variation with the trapped charge carriers concentration after irradiation (n_0); figure (b) shows the difference with the energy of activation (E); (c) shows the difference with the escape frequency (s); figure (d) explains the difference with the heating rate (β). The values of the parameter: (n_0=1 m^{-3}) , (E=1 eV) ; (s=1×10^{12} s^{-1}) , (β=1 K/s) the other parameters are remaining constant when varied one parameter [8].

$$I(T) = \frac{n_0^2}{N}\frac{s}{\beta}\exp\left\{-\frac{E}{kT}\right\}\left[1+\frac{n_0 s}{N\beta}\int_{T_0}^{T}\exp\left\{-\frac{E}{kT'}\right\}dT'\right]^{-2} \qquad (2.15)$$

The above equation (2.15) is the equation of the (Garlick–Gibson) thermoluminescence (TL) for the kinetics of the second-order. The peak approximately symmetric and high temperature part is slightly wider than low temperature part of curve. And it could be seen from the fact that in a 2nd order process the great amount of releasing electrons trapped again before recombination, and it has led to a delay in the luminescence emission over the range of broader temperature. The initial value of n_0 shows here not just as a multiplicative constant as

in the case of 1st order, the variation in different dose levels is the reason of changing the curve shape. This is explained in the figure (2.4 (a)). As it is seen T_m decreases when n_0 increases. The temperature change can be derived [29] and proximated by the following equation;

$$T_1 - T_2 \approx T_1 T_2 (\frac{k}{E}) \ln f \tag{2.16}$$

T_1 is the temperature of the maximum intensity at a specific dose and (T_2) is the temperature of the maximum intensity at (f) times higher dose. And the parameter values in the figure (2.4(a)) the shift is (25 K). Figure 2.4b describes the difference in position and size of a 2nd order peak as a function of E. In the figure 2.4c (s) is a function of the (s/N), and in the figure (2.4(d)) as a function of the heating rate (β). As in the case of the first-order kinetics, the area under the curve is proportional to the initial concentration (n_0) but the peak height is no longer directly proportional to the peak area, despite the small deviation.

It can be noted that, in the1st order case, the temperature dependence in the initial rise is (exp(-E/kT)). Also can be applied here the initial rise way for calculating the trap depth and for the kinetics of the 2nd order the shape of the glow peak, the equation 2.15 can be approximated with a function written in terms of intensity of the maximum peak (I_m) and the the maximum temperature of peak (T_m) [10].

$$I(T) = 4I_m \exp(\frac{E}{kT}\frac{T-T_m}{T_m}) \times \left[\frac{T^2}{T_m^2}(1-\Delta)\exp\left\{\frac{E}{kT}\frac{T-T_m}{T_m}\right\} + 1 + \Delta_m\right]^{-2} \tag{2.17}$$

Where ($\Delta = \frac{2kT}{E}$) and ($\Delta_m = \frac{2kT_m}{E}$)

2.2.3 General-order kinetics

The forms of the 1st order and the 2nd order of the equation of the thermoluminescence (TL) have been acquired by using the exact, simplifying

expectations. However, the peak of the thermoluminescence (TL) will commensurate neither kinetics of the first-order nor the kinetics of the second-order at the time which are do not hold these simplifying assumptions. May and Partridge [6] used in the case of General-order kinetics an experimental expression for the kinetics of the general-order (TL), and this is.

$$I(t) = -\frac{dn}{dt} = n^{b} s' \exp\left\{-\frac{E}{kT}\right\} \tag{2.18}$$

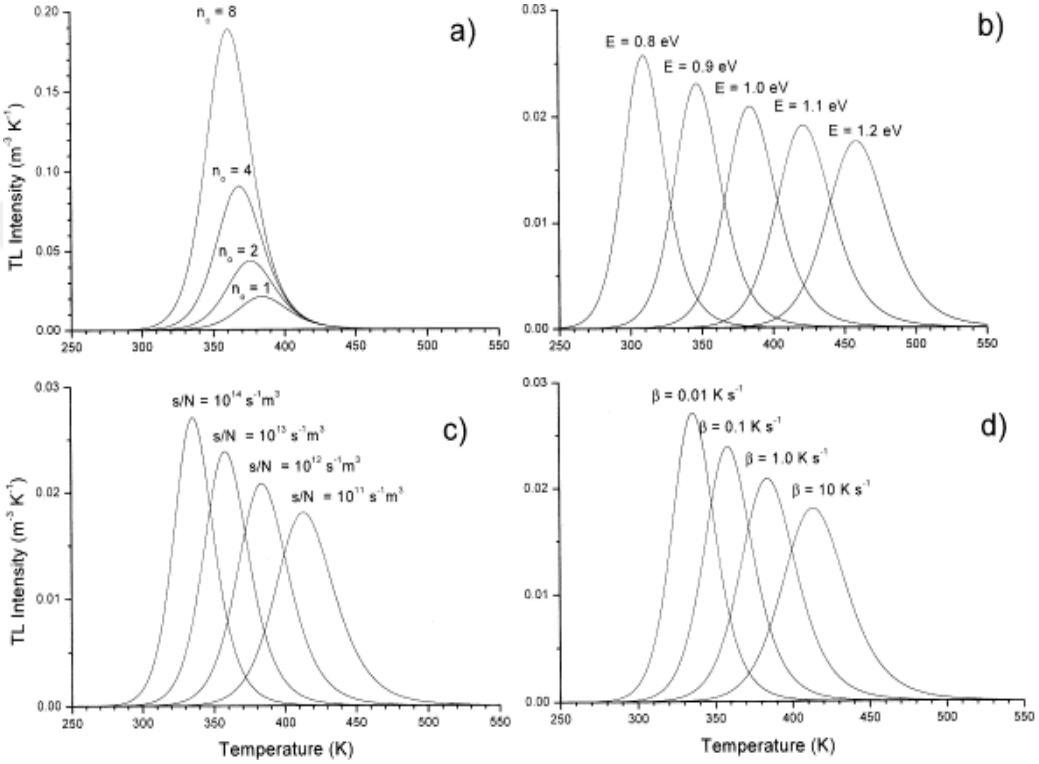

Figure 2.4 The properties of Garlick–Gibson second-order kinetic equation of the thermoluminescence (TL) [8]

Integration of the equation (2.18) for ($b \neq 1$) yields:

$$I(T) = \frac{s''}{\beta} n_0 \exp\left\{-\frac{E}{kT}\right\}\left[1 + (b-1)\frac{s''}{\beta}\int_{T_0}^{T} \exp\left\{-\frac{E}{kT'}\right\} dT'\right]^{-b/(b-1)} \tag{2.19}$$

Where ($s''=s' n_0^{b-1}$) is in unit (s^{-1}). The equation.(2.19) includes the case of second-order (b=2) and changes to the equation.(2.10) when ($b \rightarrow 1$). However, the case of the general-order is useful for intermediate cases can be dealt with and it running smoothly to the first-order when ($b \rightarrow 1$) and to the second-order when ($b \rightarrow 2$), look the figure 2.5.

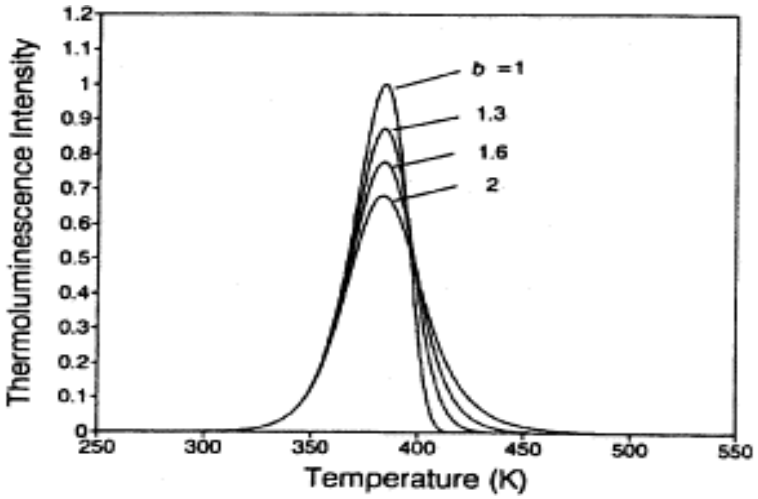

Figure 2.5 The differences between the first-order, second-order and intermediate-orders of TL peaks [8].

2.2.4 Advanced models

The OTOR model (one trap-one center) explains whole properties of the thermoluminescence phenomenon and interprets the behavior of the glow peak shape in accordance with the difference of the radiaiton dose and rate of heating (β). And thus, there isn't any thermoluminescence substance which is defined by the simple model. It can not be said that this model has no significance. But in opposite it has helped us to interpret a lot of features that can be considered like the variations of the OTOR model [1]. Here, it is very briefly mentioned only some models in order to get an idea of the complexity of this phenomenon in the real thermoluminescence substance. Generally, it will appear more than a single electron trap of real thermoluminescence material and it is not to be active all the traps in the range of temperature in which the sample is heated. The trap, that can be filled with electrons during radiation is called the thermally disconnected the trap. Trapped electrons in the deeper levels are not affected during the heating process as shown in figure 2.6a. It is said that (DET) is disconnected thermally. But its presence has an impact on the trapping filling and ultimately on the glow peak shape. [8].

Suppose that the trapped electrons are released while the sample heated, but the trapped holes are staying in the recombination center. And thus, can be changed this status after the release of an electrons and holes at the same time from their traps and at the same period of temperature, and in thermally will release the holes from the same centers and operating as sites of recombination of the thermally freed electrons

and vice versa, look the figure (2.6 (b)). The equation (2.2) is invalid in this case. And should be formulated new differential equations. The analysis of this complex kinetic sample detects a glow curve it reserves the simple 1st order equation 2.11 or 2nd order equation 2.16, depending on the selected values of the parameters. However, the (E) and (s) values used in the equation (2.11) and equation (2.16). For getting this model a suitable on this complex kinetics require additional explanation and there is another process that could be occur is a process of recombination without transition of an electron into the (C.B) (see figure (2.6 (c)). When allow a transition of an electron into the center of recombination, the electron is thermally trigdred into an excited level. And this means that trap is near the center.

The probability of transition may deeply depend on the distance between the two centers. It can be found a statement for the intensity of the (TL) by a certain assumptions [1]. Finally, we can remind the possibility that the defect isn't stable but engaged with another defect interaction, the figure (2.6 (d)) while the concentration of the trapped electron is stable at low temperature the result may be that the depth of the trap will change. And the electrons are participating in two processes at higher temperature: firstly, is the escape of electrons to the (C.B), secondly, is the reaction of the defect [2].

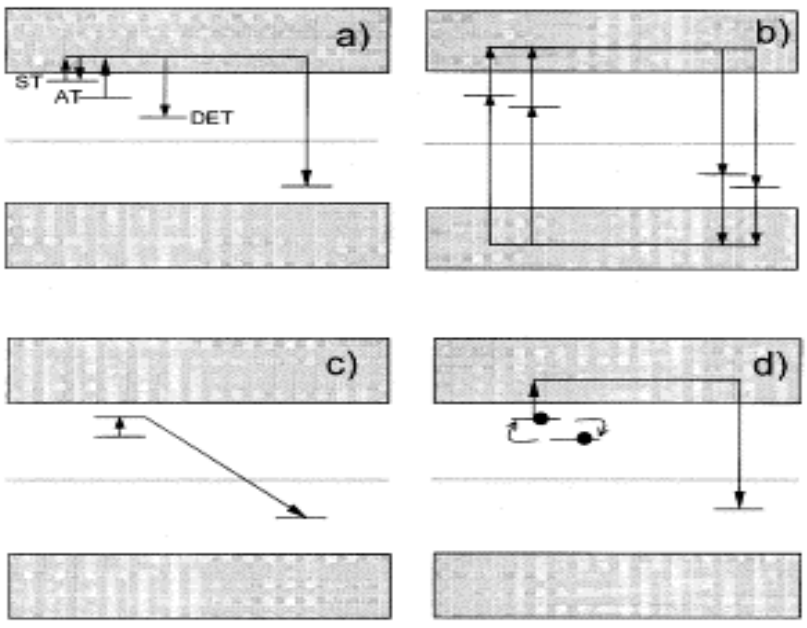

Figure 2.6 Advanced models describing the thermally stimulated release of trapped charged carriers [8].

2.3 Trapping Parameter Determination Methods

There are different ways to assess the parameters of the trapping from the glow curves. And the calculation of the trap parameters from the curves is the main concern for a long time [19,20]. The initial rise (IR), heating rate (HR), and peak shape (PSM) methods will be appropriate ways for determining these parameters. If there are complex peaks; the partial thermal cleaning method and the the computer glow curve deconvolution (CGCD) program will be usefull fort he correct determination of the values. In many cases, it cannot be used the partial thermal cleaning way for isolating the interest peak completely without making any perturbation on it. Therefore, (CGCD) program become so popular way to assess the trap values from thermoluminescence glow curves [21,22].

2.3.1 Peak Shape (PS) Method

The peak shape method was firsly established by Chen [33], later Halperin and Braner's adjusted the equations [35] to calculate the values of (E);

$$E_\tau = \left[1.51 + 3(\mu_g - 0.42)\right]\frac{kT_m^2}{\tau} - \left[1.58 + 4.2(\mu_g - 0.42)\right]2kT_m$$
$$E_\delta = \left[0.976 + 7.3(\mu_g - 0.42)\right]\frac{kT_m^2}{\delta}$$
$$E_\omega = \left[2.52 + 10.2(\mu_g - 0.42)\right]\frac{kT_m^2}{\omega} - 2kT_m$$

(2.20)

After selecting the activation energy and the kinetic order, using the following expressions (s) frequency factor, it must be observed that this parameter called as pre-exponential factor in the general order kinetic, can be appreciated for first and general order kinetics respectively.

$$s = \frac{\beta E}{kT_m^2}\ \exp\left[\frac{E}{kT_m}\right]$$
$$s = \frac{\beta E}{kT_m^2}\left[\exp(-\frac{E}{kT_m})(1 + (b-1)\frac{2kT_m}{E})\right]^{\frac{b}{b-1}} \qquad (2.22)$$

2.3.2 CGCD Method

Computer based glow curve deconvulation (CGCD) method has some advantages over the experimental ways since it does not required any heating process. And it is also one of the most important technique to find the trapping values. The glow-curve deconvolution (CGD) technique is very popular during for a long time [21,22].

For the first order glow curve the following expression is used;

$$I(T) = n_0 s \quad \exp(-\frac{E}{kT})\exp\left[(-\frac{s}{\beta}\frac{kT^2}{E}\exp(-\frac{E}{kT}) * (0.9920 - 1.620\frac{kT}{E_a})\right] \qquad (2.23)$$

For the second order glow curve the following expression is used,

$$I(T) = n_0 s \quad \exp(-\frac{E}{kT})\left[1 + (-\frac{(b-1)s}{\beta}\frac{kT^2}{E}\exp(-\frac{E}{kT}) * (0.9920 - 1.620\frac{kT}{E_a})\right]^{\frac{b}{b-1}} \qquad (2.24)$$

Where I(T) is the fitted total glow curve, (a) allows for the contribution of the electronic noise to the contribution of the planchet and dosimeters infrared to the background. Starting from the equation (2.25), the procedure of the least square minimization and also the figure of Merit (FOM) was used for judging the fitting results on whether they are good or not. Like,

$$FOM = \sum_{i=1}^{n} \frac{\left|N_i(T) - I(T)\right|}{A} = \sum_{i=1}^{n} \frac{\left|\Delta N_i\right|}{A} \qquad (2.25)$$

Where ($N_i(T)$) is the i-th experimental points (total n=200 data points), ($I(T)$) is the i-th fitted points, and (A) is the integrated area of the fitted glow curve.

In many experiments [22].It can be said that if the the (FOM) values are between (0.0%) and (2.5%) the fit is good, if the (FOM) values between (2.5 %) and (3.5%) the fit is fair, and if the (FOM) values is greater than (3.5%) the fit is bad. To have a graphic representation of the agreement between the experimental and fitted glow curves, the computer program also plots the function,

$$X(T) = \frac{N_i(T) - I_i(T)}{\sqrt{I_i(T)}} \tag{2.27}$$

which is a normal variable with an expected value (0) and (σ =1) where ($\sigma^2(T)=I_i(T)$).

2.3.3 Initial Rise Method (IRM)

The method of the initial rise (IRM) is the most generally applicable way and also the simplest way to assess the energy of the activation (E) of a single peak of the thermoluminescence (TL). The fundamental hypothesis underlying this way is that at the end of low temperature peak, each relating occupancies of the states, the trap, the center of recombination and, sometimes, can be considered other interactive states as being almost constant, thus:

$$I(T) = C\exp(-E/kT) \tag{2.28}$$

A linear plot is obtained with slope equal to *(–E/k)* by drawing ln *(I)* against *(1/T).* Therefore, that it is easy to assess the activation energy *(E)* without frequency factor knowledge as shown in the equation below.

$$E = -kd(\ln(I))/d(1/T) \tag{2.29}$$

The activation energy (E) was got from the above equation, and then we can get the frequency factor (s) as shown in this equation

$$\frac{\beta E}{kT_m} = s\exp(-\frac{E}{kT}) \tag{2.30}$$

Where the *(β, E, k, T)* is the heating rate, activation energy, Boltzmann constant, absolute temperature, respectively. And (T_m) is the maximum intensity temperature. But can be used this way only in those cases when a peak is glow clearly defined and clearly separated from other peaks.

2.3.4 Heating Rate Method (HRM)

Various heating rates are another important method to determine E, and the peak temperatures will be different when heating the sample at two various heating rates (β_1) and (β_2).

The above equation (2.30) can also be written as;

$$E = k\frac{T_{m1}T_{m2}}{T_{m1}-T_{m2}}\ln[(\frac{\beta_1}{\beta_2})(\frac{T_{m2}}{T_{m1}})^2] \tag{2.31}$$

The main feature of the method of the heating rate is that it only needs data that should be yielded at a maximum peak (T_m, I_m). Moreover the problems which are due to thermal quenching, are not effect on the calculation of E as with the initial rise method (IRM).

When the various heating rates are used for the 1st order kinetics the expression can be obtained as:

$$\ln(\frac{T_m^{\ 2}}{\beta}) = (\frac{E}{k})(\frac{1}{Tm}) + cons\tan t \tag{2.32}$$

If ln (T_m^2/β) against ($1/T$) is plotted a linear curve will be obtained having a slope of (E/k). Then E could be evaluated from the slope. In addition, if one extrapolated $1/T_m = 0$ frequency factor s could be found. This different heating rate technique is applicable to general-order kinetics which contains the second-order case. For the general order case, one can plot ($ln\left[I_m^{\ b-1}(T_m^{\ 2}/\beta)^b\right]$) against ($1/T_m$), whose slope is equal to (E/k).

CHAPTER 3

EXPERIMENTAL PROCEDURE

In this chapter, it's described the experimental procedure, equipment, and the way that material achieved and produced.

3.1 Experimental Procedure and Equipment

Before next irradiation, the samples were first annealed to wipe any remaining information. For this reason, $CaMoO_4$: Eu^{+3} was annealed at 300 ± 1 ^oC for thirty minutes. Thermal treatments were done with microprocessor- controlled oven of within ± 1.0 ^oC. The samples were irradiated at room temperature with beta source (^{90}Sr-^{90}Y). The activity of the β-source is about 100 mCi. The recommended working lifetime is about fifteen years. Strontium–90 emits high - energy beta particles from their daughter products (^{90}Sr β-0.546 MeV together with ^{90}Y β-2.27 MeV). Beta radiation is absorbed by air, so its intensity reduced with distance much More quickly than inverse square law calculations would indicate. The maximum range of Y–90 beta particles in air is approximately 9 meters. The average strength of a 100 mCi Sr–90 β-source is 2.64 Gy/minute=0.0438 Gy/sec for fine grains of aluminium [21]. After the irradiation process the samples were read out by using Harshaw QS 3500 manual type reader that is connected to a computer. It economically provides high reliability. The basic block diagram of reader is illustrated obviously in the figure 3.1. A clear glass standard filter was placed between the planchet and photomultiplier tube to get rid of the unwanted infrared light. The instrument includes a sample change drawer for inserting and removing the TLD elements. The reader has the capability of increasing temperature up to 400 ^oC for different linear heating rates between 1 $^oC/s$ to 50 $^oC/s$ within ± 1 ^oC error [23].

Figure 3.2 shows the profile of the typical time temperature. For improving the low-exposure reading accuracy and to extend planchet life, the 3500 provides for nitrogen to flow around the planchet. Through the elimination of oxygen in the salinity, flow of nitrogen eliminates unwanted TL signal caused by the oxygen. Nitrogen is also directed through the photo-multiplier tube (PMT) chamber to eliminate moisture caused by condensation.

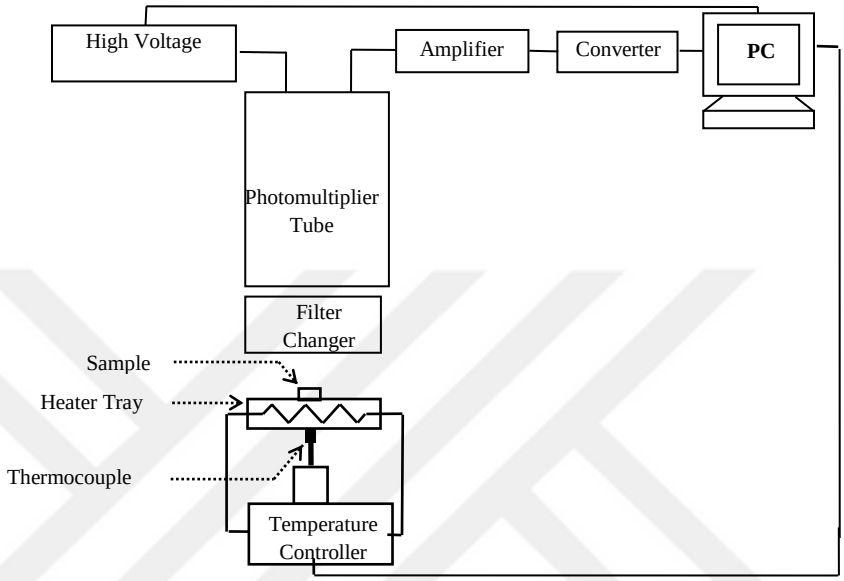

Figure 3.1 Basic block diagram of TL reader [23].

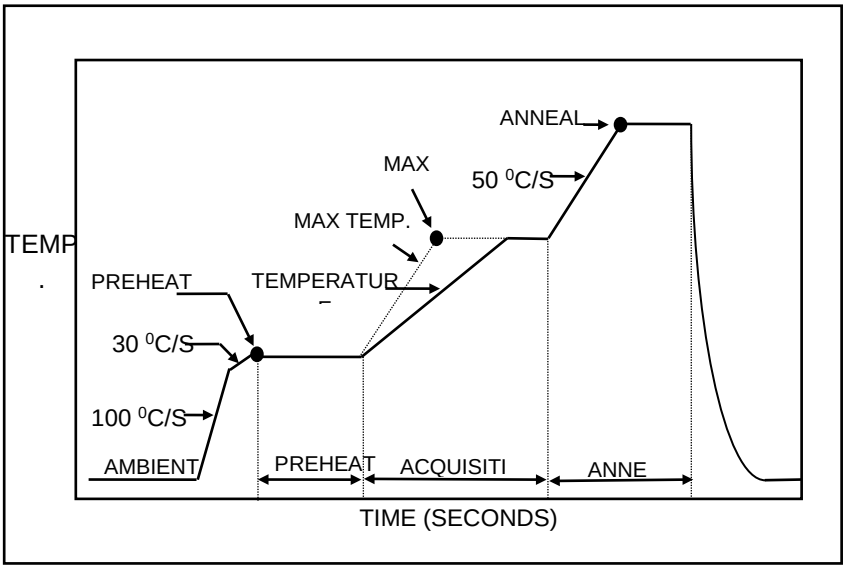

Figure 3.2 Typical time temperature profile (TTP) [23].

(a)

(b)

Figure 3.3 Experimental equipments (a) ^{90}Sr-^{90}Y β-source & 9010 Optical Dating System (b) Harshaw TLD System 3500.

3.2. Synthesis of Europium doped Calcium Molybdate ($CaMoO_4:Eu^{+3}$)

3.2.1. Materials

The raw materials used in this study were MoO_3, $Ca(NO_3)_2$, Eu_2O_3 (Merck-without further purification).

3.2.2. Synthesis

Calcium Molybdate ($CaMoO_4$: Eu^{+3}) was prepared by the complex polymerization method (CPM). In this method, molybdate citrate was formed by dissolution of MoO_3 and citric acid in aqueous solutions. The citrate solution was well homogenized under constant stirring at a temperature of ~ 60-80°C. After achieving complete dissolution was add stoichiometric amounts of $Ca(NO_3)_2$.

The complex was well stirred for several hours at 80–90°C to produce a clear, homogeneous solution. After the solution was homogenized, ethylene glycol was added to promote the polyesterification. With continued heating the viscosity of the solution increased, albeit devoid of any visible phase separation. After partial evaporation of the water, the resin was heat treated at 300°C for 2 h, in a static oxidizing atmosphere, leading to the partial decomposition of the polymeric gel, forming an expanded resin, constituted of partially pyrolyzed material. This pre-pyrolyzed material was removed from the furnace and deagglomerated using mortar.

3.2.3 Characterization

The structural phase identification of $Ca_{0.95}MoO_4:0.05Eu^{3+}$ phosphor was carried out by X-ray powder diffraction (XRD) using a Bruker AXSD 8 Advance Powder Diffractometer with CuKα=1.54 Å radiation. The morphological investigations of the phosphor were carried out via a LEO440 Computer Controlled Digital Scanning Electron Microscope. Photoluminescence (PL) measurements were made by using a Varian Cary Eclipse Fluorescence spectrophotometer. PL spectra were obtained at room temperature and excitation and emission slits were arranged as 10 and 10, respectively. The $Ca_{0.95}MoO_4:0.05Eu^{3+}$ was irradiated at room temperature by beta particles from a calibrated ^{90}Sr-^{90}Y source.

The sample was read out twice and the second readout was considered to be the background of the reader plus the sample. This was subtracted from the first one and all of the analyses were carried out after the subtraction. The activity of beta source is around (100 mCi). Stronium–90 emits high - energy beta particles from their daughter products (^{90}Sr β-0.546 MeV together with ^{90}Y β-2.27 MeV). The irradiated $Ca_{0.95}MoO_4:0.05Eu^{3+}$ phosphor was read out by a reader of Harshaw QS 3500 manual type that is attached to a PC where studied and analyzed. A clear glass filter has been placed in the reader between the photomultiplier tube and planchet to eliminate the emitted infrared lights from the samples plus reader. The device contains a sample change drawer for removing and inserting the TLD elements.

3.2.4 Calculation methods

First-principle calculations were carried out using the Vienna ab-initio simulation package (VASP) [24,25] based on the density functional theory (DFT). The electron-

ion interaction was investigated as in the form of the projector-augmented-wave (PAW) method with plane wave up to on energy value of 520 eV [22,23]. For the exchange and correlation terms in the electron-electron interaction, Perdew-Burke-Ernzerhof (PBE) function [26] was used within the generalized gradient approximation (GGA).

Convergence tests were performed according to the Brillouin zone (BZ) sampling and to the size of the basis set. The converged result was achieved with 4×4×2 k-point mesh, which was used in the irreducible Brillouin zone yielding 144 k-points centered at Monkhorst–Pack for the Ca1-xEuxMoO4 compound. The special k-point mesh was produced by using the Gamma centered grid [27]. To determine the ground state geometries of the $Ca_{1-x}Eu_xMoO_4$ compounds, the conjugate gradient algorithm with force convergence less than 10^{-7} eV $Å^{-1}$ was used by minimizing stresses and Hellman–Feynman forces. The energy tolerance was found to be less than 10^{-8} eV per unit cell in the iterative solution of the Kohn–Sham equations. All steps were carried out by using Methfessel–Paxton method [28] in the order of 1 for all relaxation schemes. Then the tetrahedron methods with Blöchl corrections [29] were applied to obtain accurate energy values. Additionally, X-ray diffraction patterns were obtained by using VESTA program package [30] and the Cu Kα source having the wavelength of 1.541 Å.

CHAPTER 4

EXPERIMENTAL RESULTS AND DISCUSSION

Inorganic luminescent materials also called as phosphors can be synthesized as crystalline compounds. They can absorb energy and emit light either immediately or after a period of time. Barium sulfide first synthesized by Casciavolus in 1603 is known to be the first luminescent material. Although Casciavolus tried to obtain gold by heating certain minerals he obtained a rock emitting red light. Sulphide based luminescent materials (i.e., ZnS, CaS, BaS), which were synthesized and investigated in the mid-1800s, attracted the attention and effort of both the scientific and the industrial communities in the 1900's. However, developing sulfur-based materials with sufficient chemical stability came long after.

Synthesis of new luminescent materials and explanation of their mechanism of luminescence has been an area of great interest. The new materials with luminescence properties have gained increasing importance especially due to their enhanced optical, electronic and structural properties and due to their potential as efficient phosphors which enabled them to be preference of choice in display applications such as new flat panel displays with low-energy excitation sources, solar energy converters and optical amplifiers [31, 32]. In the last decade, tungstate and molybdate materials with scheelite and isostructural powellite structures have been widely used as hosts for trivalent rare earth ions (RE^{3+}) due to their favorable chemical, optical and structural properties [33]. Europium (III) ions have attracted much attention as it luminescence centers in red light phosphors with excellent luminescent properties [34]. Red phosphor $CaMoO_4:Eu^{3+}$, Li^+ with high PL efficiency has been extensively studies due to its potential for applications in solid state lighting [35,36] Especially when excited with UV light at 254 nm, the phosphor $CaMoO_4:Eu^{3+}$ compensated by Li^+ has a PL comparable to that of the commercial red phosphor $Y_2O_3:Eu^{3+}$ [37,38]. Moreover, various trivalent ions co-doped with Eu^{3+} in molybdates phosphors such as $CaMoO_4:Sm^{3+}$, Eu^{3+} [39], $CaMoO_4:Eu^{3+}$, Na^+

[40], $LiEu_{1-x}Bi_x(MoO_4)_2$ [41] and $NaEu(MoO_4)_2:Bi^{3+}$, Sm^{3+} [42] can also improve the luminescence property. Research on Eu^{3+} doped $CaMoO_4$ generally focused on obtaining red luminescent phosphor via various synthesis methods and increasing luminescence intensity via secondary doping ions. However, there still remains a need for studies for determining thermoluminescence properties of $CaMoO_4:Eu^{3+}$ and calculating its kinetic parameters. In this study, $Ca_{1-x}MoO_4:xEu^{3+}$ (x=0.02-0.07) phosphors were prepared and their luminescence properties were investigated. Besides this the thermoluminescence properties of $Ca_{0.95}MoO_4:0.05Eu^{3+}$ were investigated in detail after β-irradiation at room temperature and kinetic parameters, namely, the order of kinetics (*b*) and activation energy (E_a) were calculated via computerized glow curve deconvolution (CGCD) program**.**

4.1. XRD Studies

The phase purity and structural analysis of $CaMoO_4:0.05Eu^{3+}$ were made via XRD analysis. The experimental and theoretical XRD pattern of $CaMoO_4:Eu^{3+}$ are presented in Fig. 4.1. All diffraction peaks can be indexed to the Powellite structure with the space group $I41/a$ (No.88) and match well with ICDD card No: 01-077-2238. The cell parameters are $a = b = 5.217$ Å and $c = 11.414$ Å. When Eu^{3+} ions were added up to a percentage of 5% effect of doping on $CaMoO_4$ phase structure was negligible which can only be observed in small shifts in the peak positions in the XRD patterns. It is well known that the ionic radius of Eu^{3+} (1.07 Å) is close to that of Ca^{2+} (1.12 Å) in eight-fold coordination. The ionic radius of Mo^{6+}, which is 0.41 Å at coordination number is 4, is too small for to host Eu^{3+}. Therefore, Eu^{3+} ions are replaced by Ca^{2+} ions instead of Mo^{6+} ions [41]. In Figure 4.1, the XRD pattern indicates that [112] is the preferred orientation for $CaMoO_4$, for which a sharp peak at 2θ =28.300° is observed as given in Table 4.1. As can be seen in Figure 4.1 that [112] is still the preferred orientaion for small Eu^{3+} content (x=0.05), where 2θ =29.000 is measured from the experimental XRD pattern. In contrast, [101] becomes the preferred orientation when the Eu^{3+} content is high (x=0.25) and the peak apeears at 2θ = 18.290°. However as can be seen in Figure 4.1 and Table 4.1 the [112] peak is observed at 2θ =28.300.

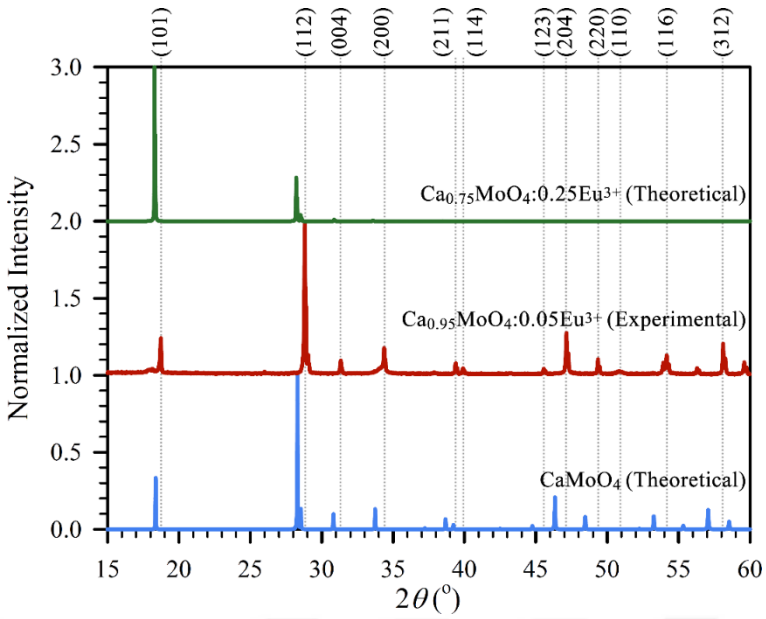

Figure 4.1 Comparison of experimental and theoretical X-Ray Diffraction (XRD) spectra of $CaMoO_4$ (bottom-theoretical) and $Ca_{0.95}MoO_4:0.05Eu^{3+}$ (middle-experimental) and $Ca_{0.75}MoO_4:0.25Eu^{3+}$ (top-theoretical).

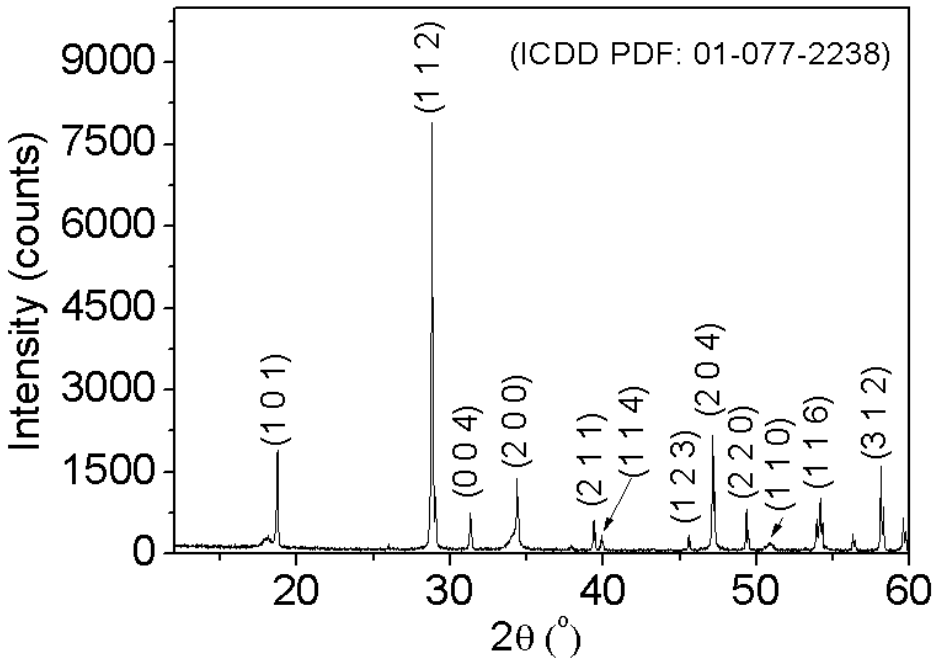

Figure 4.2. The XRD pattern of $CaMoO_4:0.05Eu^{3+}$

Table 4.1. The calculated equilibrium lattice parameters (*a* and *c* in Å) and the scattering angle (2θ) for the preferred orientation [101] of $CaMoO_4$ and [112] of $Ca_{0.75}Eu_{0.25}MoO_4$.

Compounds	Reference	*a*	*c*	E_{gap}	2θ [112]	2θ [101]
$CaMoO_4$	Theoretical	5.296	11.564	3.627	28.300	
$Ca_{0.75}Eu_{0.25}MoO_4$	Theoretical	5.335	11.580	3.379	28.300	18.290
$Ca_{0.95}Eu_{0.05}MoO_4$	Experimental (This study)	5.217	11.414		29.000	
Ca_0MoO_4:Eu	Experimental			3.7	29.000	18.300
$CaMoO_4$	Experimental	5.217	11.420	5.07		

4.2.FE-SEM/EDX Studies

FE-SEM images of the different magnification ratios of $CaMoO_4$:$0.05Eu^{3+}$ are given in figure 4.3. It is observed that the microstructure of $CaMoO_4$:$0.05Eu^{3+}$ consists of regular parallelogram planes. The average edge lengths of the parallelograms were determined in the range of 563 nm-1.463 μm. The results show that the $CaMoO_4$:$0.05Eu^{3+}$ has a good crystalline structure, so $CaMoO_4$:$0.05Eu^{3+}$ can be used in applications as high-intensity red phosphor.

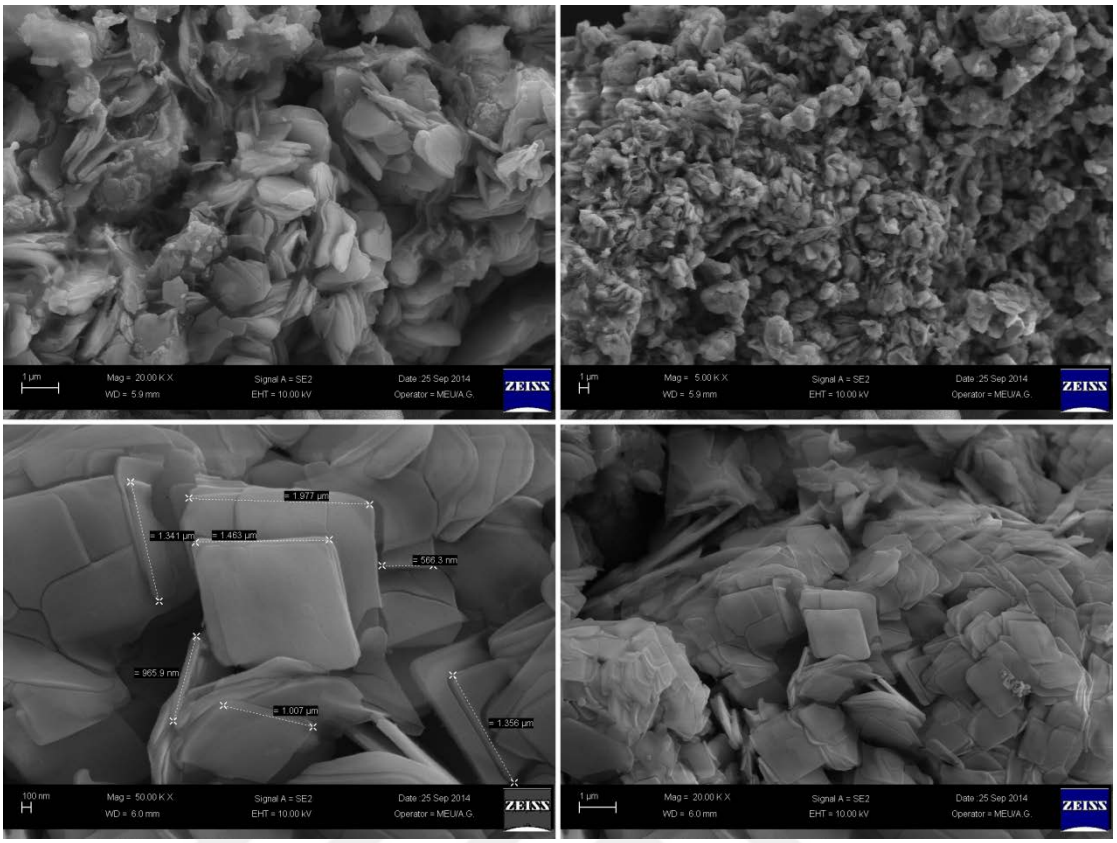

Figure 4.3 FE-SEM images of the different magnification ratios of $CaMoO_4$:0.05Eu^{3+}.

4.3. TL Results

Determination of activation energy (E_a) and frequency factor (s) mainly depends on the prior knowledge of kinetic order (b) and the exact number of glow peaks in the glow curve [1-2]. Therefore, to form an opinion about the number of glow peaks and kinetic orders (b) of all individual glow peaks in the glow curve structure of Eu doped $CaMoO_4$, the additive dose (AD) method was firstly utilized in the current study. The samples were irradiated at different doses between ≈2.4 and ≈576 Gy to check the dose dependence effect on the peak positions. Some of the selected glow curves after different dose levels are shown in Figure 4.4.

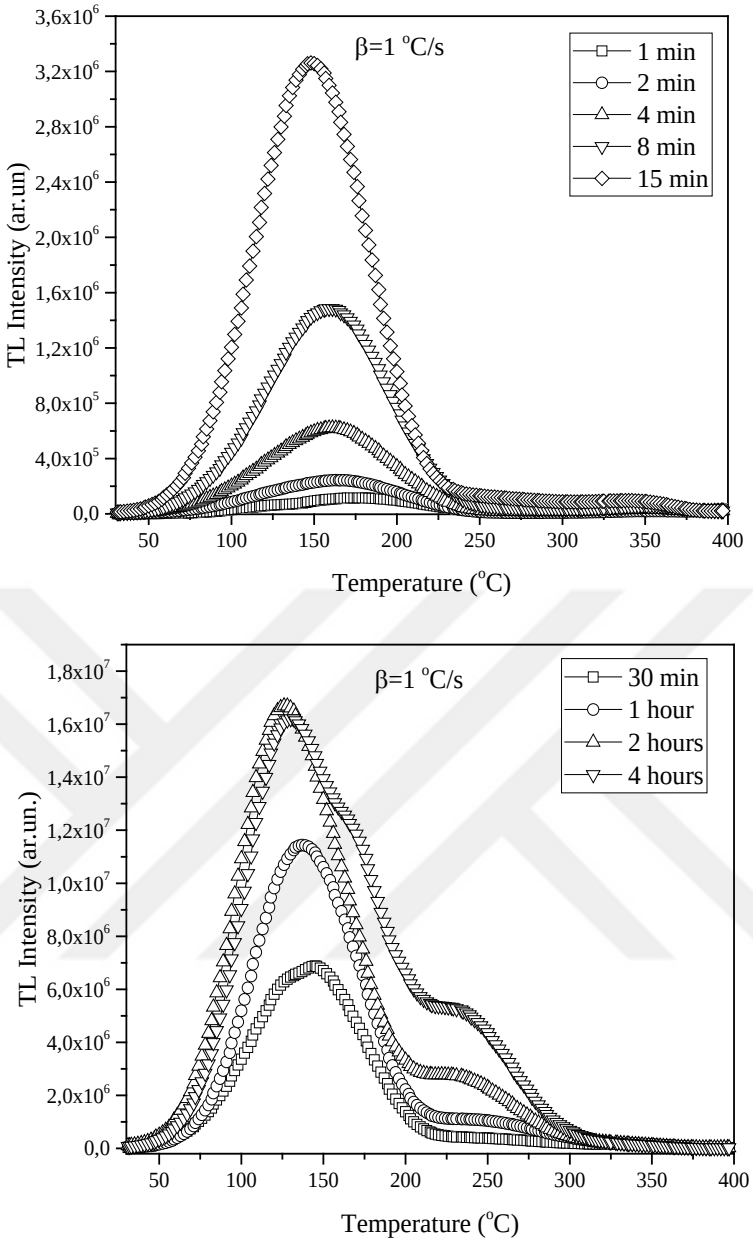

Figure 4.4 Typical glow curves of Eu doped $CaMoO_4$ exposed to β-rays from 2.4 Gy to 576 Gy at β = 1 °C.s^{-1}

The computerized glow curve deconvolution (CGCD) method has become method of preference to obtain the kinetic parameters from the glow curves of TL materials [21]. Therefore, the kinetic parameters such as number of glow peaks, activation energies (E_a) and kinetic order (b) for the dosimetric peaks of Eu doped $CaMoO_4$ were obtained by CGCD method (Fig.4.5) and are given in table 1. In this study, the following general order kinetic analytical equation was used by approximation for b≈1.1 **[**22].

$$I(T) = I_m \times b^{b/(b-1)} \times \exp\left(\frac{E}{kT} \cdot \frac{T - T_m}{T_m}\right) \times$$
$$[(b-1) \times (1 - \Delta \times \frac{T^2}{T_m^2} \times \exp\left(\frac{E}{kT} \times \frac{T - T_m}{T_m}\right) + Z_m]^{-b/(b-1)}$$

where;

$$\Delta = \frac{2kT}{E} \quad , \qquad \Delta_m = \frac{2kT_m}{E} \quad , \quad Z_m = 1 + (b-1) \cdot \Delta_m$$

Table 4.2. The values of the trapping parameters of Eu doped $CaMoO_4$

	P1	P2	P3	P4
T_{max} (°C)	97	126	152	182
E_a (eV)	0,655	0,908	0,842	1,107
b	1,20	1,66	1,26	1,86

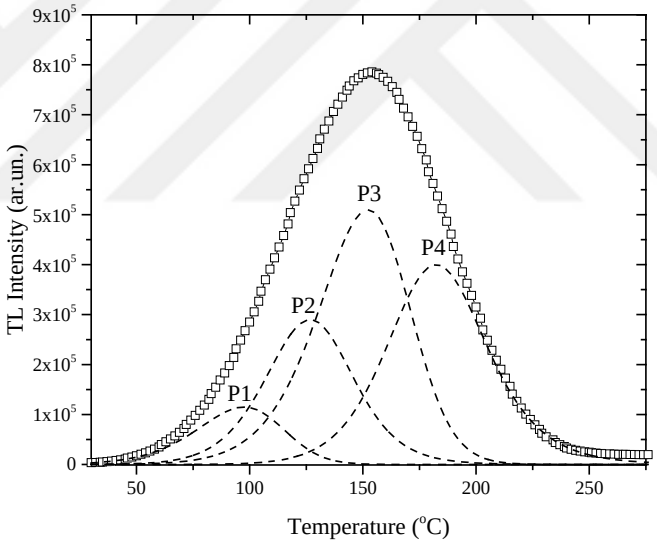

Figure 4.5 Computerised glow curve deconvolutation results for Eu doped $CaMoO_4$ measured after 12 Gy irradiation by beta ray at room temperature (β = 1 °C.s^{-1}) F.O.M = 1.11

In this study, we also evaluated the dose response function *f(D)* of Eu doped $CaMoO_4$ by using the following equation [20] to check the linearity of the samples at different dose levels.

$$f(D) = [\frac{S(D) - S_0}{D}] / [\frac{S(D_1) - S_0}{D_1}]$$

Here, D_1 is a normalization dose in the initial linear range and S_0 is the intercept on the TL intensity axis of the extrapolation of the linear region. It is seen from the figure 4.6 that, the glow curve shows linear characteristics *(f(D)=1)* at low doses, followed by a region of supralinear growth *(f(D)>1),* the curve gradually goes into a region of sublinear growth *(f(D)<1)* nearly after 10^3 Gy.

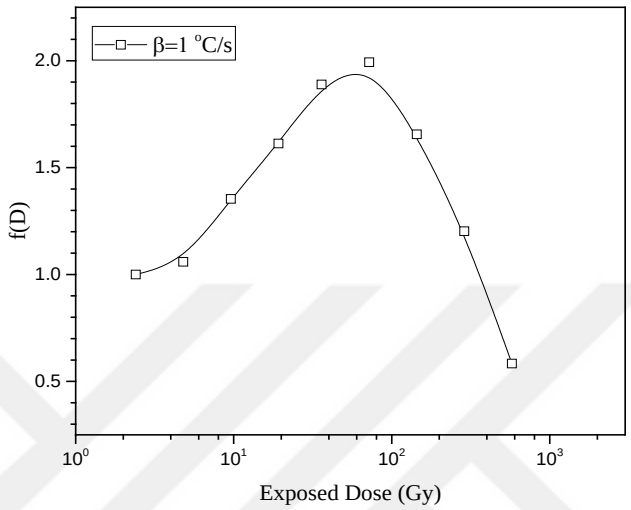

Figure 4.6 The dose response function *f(D)* vs *D* of $CaMoO_4$:Eu

Another process in this study is to understand the effect of linear heating rates on the glow curve features of $CaMoO_4$: Eu. In this section the dose response behavior of $CaMoO_4$: Eu has been investigated at different linear heating rates between 1°C to 10°C. Samples were irradiated with β-ray with a ^{90}Sr-^{90}Y source (36Gy), glow curves were recorded for different heating rates of 1, 2, 3, 5, 7, and10 °C/s, and it is shown in both of Figures 4.7 and 4.8. From these figures, it can be understood the effect of different linear heating rates were applied to the sample, thermoluminescence glow peak shifts to higher temperatures with increasing heating rate, and the width of peak increases with decreasing in maximum intensity, as expected in theory. The decreasing luminescence intensity of glow peaks as a function of the increasing heating rate is an event frequently observed in the practice of TSL. It has been recommended that it is because the effect of thermal quenching which reduces the effectiveness of the luminescence when increases temperature because of the increased non-radiative transition probability [43].

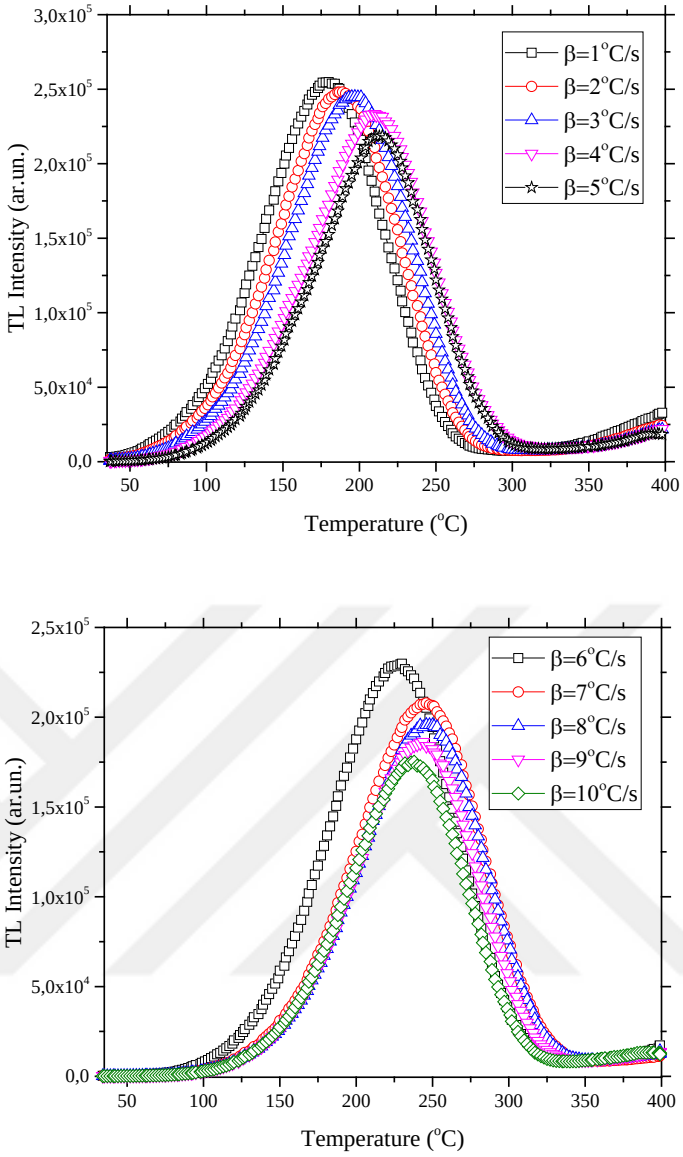

Figure 4.7 Glow curves of $CaMoO_4$: Eu measured at the different heating rates after β irradiation of 36Gy.

As a last part we have also studied in this thesis the storage time effect on the intensity of the glow peaks of Eu doped $CaMoO_4$. For this experiment, the material was irradiated up to 36 Gy. The storage time experiments were performed for different time periods. The figure 4.8 shows the measured glow curves at the end of the scheduled storage periods. As shown from the figure 4.9 the total peak area of $CaMoO_4$: Eu at the end of the scheduled storage times reduced typically 40 % of its original value.

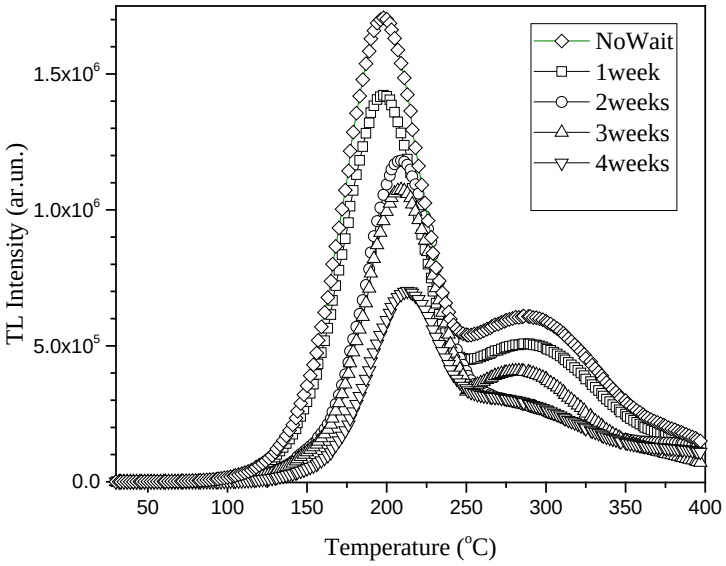

Figure 4.8 Thermoluminescence glow curves of $CaMoO_4$:Eu after various storage periods at RT after exposing to an irradiation of 36 Gy.

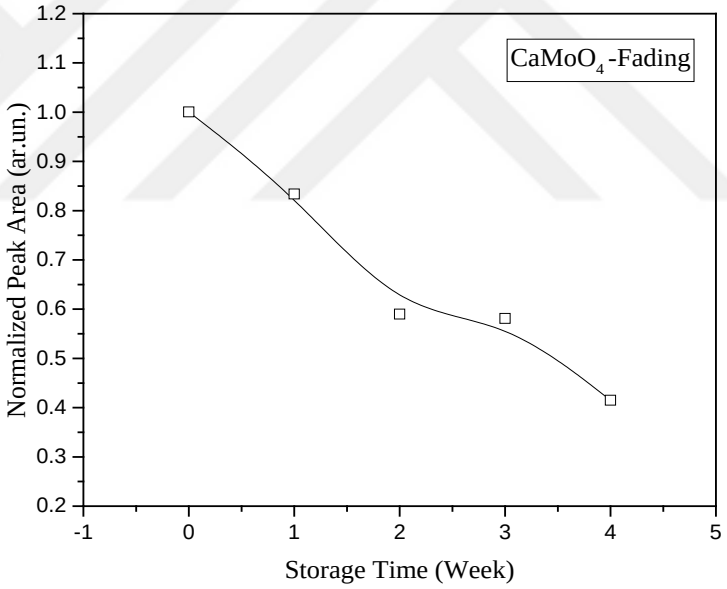

Figure 4.9 Normalized TL intensity of $CaMoO_4$:Eu after different storage times at room temperature. (β=1 $^oC.s^{-1}$ and D=36 Gy)

CHAPTER 5

CONCLUSION

Long afterglow phosphors are types of energy storing materials, which can absorb energy under excitation sources such as sunlight or an artificial lamp, and gradually emit the absorbed energy by means of visible light after the excitation source is turned off. These materials have been widely used for emergency signing, decorative purposes, traffic signs and escape route indicators [44]. In recent years, the optical properties of trivalent rare-earth ions (RE^{3+}) in tungstate and molybdate materials with scheelite and isostructural powellite structures have been widely investigated. Especially, many researchers focused their attention on europium (III) ions as luminescence centres in red light phosphors with excellent luminescent properties [45]. $CaMoO_4$ with a scheelite type structure has been of practical interest for a long time because of its attractive luminescence [46]. It provides green emission as an available solid-state laser material. $CaMoO_4$ belongs to the family of the tungstate's and molybdates having general formula MXO_4 (M = Ca, Sr, Ba; X = W, Mo) and scheelite structure. These crystals have been reported to be good host lattices for lasing ions on one hand, and suitable materials for the development of Raman lasers on the other. The absorption (360–1900 nm) and emission (460–850 nm) spectra and the decay curves of the luminescence were measured at temperatures ranging from 10 to 298 K [47].

In this study we have investigated the thermoluminescence properties of Eu doped $CaMoO_4$ in detail after β-irradiation at room temperature and kinetic parameters namely the order of kinetics (*b*), activation energy (E_a) were calculated using the computerized glow curve deconvolution (CGCD) program**.** The specimens were irradiated at room temperature by beta particles from a calibrated ^{90}Sr-^{90}Y source. At each experimental measurement, four samples were read out. Each sample was read out twice and the second readout is considered to be the background of the reader plus sample; this was subtracted from the first one and all of the analyses have been carrier out after the subtraction. The activity of beta source is around (100 mCi).

Stronium–90 emits high- energy beta particles from their daughter products (^{90}Sr β-0.546 MeV together with ^{90}Y β-2.27 MeV). The irradiated specimens were read out by a reader of Harshaw QS 3500 manual type that is attached to a PC where studied and analyzed. A clear glass filter has been placed in the reader between the photomultiplier tube and planchet to eliminate the emitted infrared lights from the samples plus reader. The device contains a sample change drawer for removing and inserting the TLD elements. The determination of activation energy (E_a) and frequency factor (s) mainly depends on the prior knowledge of kinetic order (b) and the exact number of glow peaks in the glow curve [1]. Therefore, to form an opinion about the number of glow peaks and kinetic orders (b) of all individual glow peaks in the glow curve structure of Eu doped $CaMoO_4$; the additive dose (AD) method was firstly utilized in the current study. The computerized glow curve deconvolution (CGCD) method has become very popular way to obtain the kinetic parameters from the glow curves of TL materials [21, 22]. Therefore, the kinetic parameters such as number of glow peaks, activation energies (E_a) and kinetic order (b) for the dosimetric peaks of Eu doped $CaMoO_4$ were obtained by CGCD method. A careful investigation of this figure indicates that glow curve structure of the sample is described by a linear combination of at least four glow peaks between RT and 400 ^oC when the glow curve is immediately recorded after irradiation and also a best fit was always obtained by assuming that the P1 (T_{max} (^oC)=97), P2 (T_{max} (^oC)=126), P3 (T_{max} (^oC)=152), P4 (T_{max} (^oC)=182), is of general-order kinetics and the other peaks. The peaks have activation energies 0,655 eV, 0,908 eV, 0,842 eV and 1,107 eV respectively. The computed trapping parameters are presented in table 4.2. As a last part we have also studied in this thesis the storage time effect on the intensity of the glow peaks of Eu doped $CaMoO_4$. For this experiment, the material was irradiated up to 36 Gy. The storage time experiments were performed for different time periods. For this experiment, the material was irradiated up to 36 Gy. The storage time experiments were performed for different time periods. In Figure 12 are shown the glow curves measured at the end of the scheduled storage periods. As shown in Figure 13 the total peak area of $Ca_{0.95}MoO_4:0.05Eu^{3+}$ at the end of the scheduled storage times reduced typically to 40 % of their original value. To solve this problem, we recommend adding multiple co-dopants to the host lattice.

REFERENCES

[1] McKeever S.W.S. 1985. Thermoluminescence of Solids. Cambridge University Press, Cambridge.

[2] McKeever S.W.S., Moscovitch M. and Townsend, P.D. 1995. Thermoluminescence Dosimetry Materials: Properties and Use. Nuclear Thechnology Publishing.

[3] Mahesh K., Weng P.S. and Furetta C. 1989. Thermoluminescence in Solids and its Applications. Nuclear Technology Publishing Ashford.

[4] Randall, J.T. and Wilkins, M.H. F. (1945). Phosphorescence and electron traps: II. The interpretation of long-period phosphorescence. *Proceedings of the Royal Society A.* **184**, 390-407.

[5] Garlick, G.F.J and Gibson, A.F. (1948). The electron trap mechanism of luminescence in sulphide and silicate phosphors. *Proceedings of the Physics Society*. **60**, 574-589.

[6] May, C.E. and Partridge, J.A. (1964). Thermoluminescence kinetics of alpha irradiated alkali halides. *Journal of Chemical Physics*. **40**, 1401-1415.

[7] McKeever S W S (1984). Thermoluminescence in Quartz and Silica. *Radiation Protection Dosimetry*. ***8***, 81.

[8] Chen R and McKeever S W S, 1997. Theory of Thermoluminescence and Related Phenomena. World Scientific, Singapore.

[9] Townsend, P.D., and Kelly, J.C. 1973. Colour Centers and Imperfection in Insulator and Semiconductors. London, Chatto and Windus for Sussex University Press.

[10] Hwang F. S. W.. (1972). Evaluation of the Thermoluminescence Dating Technique Applied to Smoky Quartz. *Journal of Geophysical Research*. ***77***, 328.

[11] Mattern P. L., Lengweiler K. and Levy P. W. (1975). *Radiation Effects and Defects in solids*. **26**, 237.

[12] Furetta, C., and Kitis G. (2004). Review models in thermoluminescence. *Journal of Materials Science*. **39**, 2277.

[13] Schwartzman R. G., Kiersted J. A. and Levy P. W., (1983), Thermoluminescence of the Mineral Components in Granite. *PACT*. **9**, 16.

[14] Chen R., Yang X. H. and McKeever S. W. S., (1988). Strongly Superlinear Dose Dependence of Thermoluminescence in Synthetic Quartz. *Journal of Physics D: Applied Physics*. **21**, 1312.

[15] Petrov S. A. and Bailiff I. K., (1995). The 110.Degrees-C TL Peak in Synthetic Quarz, Radiation *Meas*urements. **24**, 519.

[16] Horowitz Y. S. and Yossian D., (1995). Computerised glow Curve Deconvolution: Application to Thermoluminescence Dosimetry. *Radiation Protection Dosim*etry. **60**, 1.

[17] J.K. Srivastava, B.C. Bhatt and S.J. Supe, (1992). Thermoluminescence Characteristics of $CaSO_4$ Doped with Dy and Cu. *Radiation Protection Dosim*etry. **40**, 271.

[18] T. Yamashita, T., Nada, N., Onishi, H., and Kitumura, (1971). Calcium Sulfate Activated by Thulium or Dysrosium for Thermoluminescence Dosimetry. *Healt Physics*. **21**,295.

[19] Kitis G., Pagonis V., Carty H. and Tatsis E., (2002). Detailed Kinetic Study of the Thermoluminescence Glow-Curve of Synthetic Quartz. *Radiation Protection Dosimetry*. **100**, 225.

[20] Pagonis V., Tatsis E., Kitis G., Drupieski C. (2002). Search for Common Characteristics in the Glow-Curves of Quartz of Various Origins. *Radiation Protection Dosimetry*. **100**, 373

[21] Bos A. J. J., Piters J. M., Gomez Ros J. M. and Delgado A., GLOCANIN, and Intercomparision of Glow Curve Analysis Computer Programs IRI-CIEMAT Report, 131-93-005 IRI Delft, (1993).

[22] Kitis G., Gomez Ros J.M., and Tuyn J. W. N. (1998) Thermoluminescence glow-curve deconvolution functions for first, second and general orders of kinetics. *Journal of Physics D: Applied Physics*. **31,** 2636.

[23] 9010 Optical Dating system User Manuel, Dec. 1993.

[24] G. Kresse. (1999). From ultrasoft pseudopotentials to the projector augmented-wave method. *Physical Review B*. **59**. 1758–1775.

[25] P.E. Blöchl.(1994). Projector augmented-wave method. *Physical Review B*. **50**, 17953–17979.

[26] J.P. Perdew, K. Burke, M. Ernzerhof. (1996). Generalized Gradient Approximation Made Simple. *Physical Review Letters.* **77**, 3865–3868.

[27] H. Monkhorst, J. Pack.(1976). *Physical Review B*. **13**, 5188.

[28] M. Methfessel, A.T. Paxton. (1989). High-precision sampling for Brillouin-zone integration in metals**.** *Physical Review B*. **40**, 3616–3621.

[29] P.E. Blöchl, O. Jepsen, O.K. Andersen. (1994). Improved tetrahedron method for Brillouin-zone integrations. *Physical Review B*. **49**, 16223–16233.

[30] K. Momma, F. Izumi, P.M. J., P.C. J., H.P. J., C.S. J., P.M. C., N. T., K. Y. (2011). *VESTA 3* for three-dimensional visualization of crystal, volumetric and morphology data, *Journal of Applied Crystallography*. **44,** 1272–1276.

[31] C. Cheng, C. Tang, X.X. Ding, X.T. Huang, Z.X. Huang, S.R. Qi, L. Hu, Y.X. Li. (2003). Catalytic synthesis of aluminum borate nanowires, *Chemical Physics Letter*. **373,** 626e629.

[32] B.B. Shachar, Y. Laichter, U. German, G. Weiser. (1986). An improved energy compensating holder for CaF_2:Dy TLD crystals used for environmental measurements, *Radiation Protection Dosimetry*. **12** (4) ,333e337.

[33] S.J. Lei, X.M. Peng, X.P. Li, Z.H. Liang, Y. Yang, B.C. Cheng, Y.H. Xiao, L. Zhou. (2011). *Materials Research Bulletin*. **46**, 601.

[34] Gediminas BRAZIULIS, Ruta STANKEVICIUTE, Arturas ZALGA.(2014). Sol-gel Derived Europium Doped CaMoO4:Eu^{3+} with Complex Microstructural and Optical Properties. MATERIALS SCIENCE Vol. 20, No. 1.

[35] P.P. Yang, C.X. Li, W.X. Wang, Z.W. Quan, S.L. Gai, J. Lin, J.(2009). *Solid Sate Chem*. **182**, 2510.

[36] Z.G. Xia, S. Jin, J.Y. Sun, H.Y. Du, P. Du, L.B. Liao, J. Nanosci. (2011). *Nanotechnol*. **11**, 9612.

[37] F.Y. Yua, J. Zuo, Z. Zhao, C.Y. Jiang, Q. Yang. (2011). Low temperature synthesis and photoluminescent properties of CaMoO4:Eu3+ red phosphor with uniform micro-assemblies. *Material Research Bulletin*. **46**, 1327.

[38] F. Lei, B. Yan. (2008). Hydrothermal synthesis and luminescence of $CaMO_4$:RE^{E+}(M=W, Mo; RE=Eu, Tb) submicro-phosphors. *Journal of Solid State Chemistry*. **181**, 855.

[39] Y. Jin, Z.D. Hao, X. Zhang, Y.S. Luo, X.J. Wang, J.H. Zhang. (2011). Dynamical processes of energy transfer in red emitting phosphor $CaMoO_4$:Sm^{3+}, Eu^{3+}. *Optical Materials*. **33**, 1591–1594.

[40] M.J. Kim, Y.D. Huh. (2012). Synthesis and optical properties of CaMoO4:Eu^{3+}, Na^{+} nanophosphors and a transparent $CaMoO_4$:Eu^{3+}, Na^{+} suspension. *Optical Materials*. **35**, 263–267.

[41] J.L. Lei, Y. Yu, L.J. Li, S.B. Cheng, G.Y. Li, N.B. Li. (2012). Synthesis of $LiEu_{1-x}Bi_x(MoO_4)_2$ red phosphors by sol-gel method and their luminescent properties. *Journal of Rare Earths*. **30**, 330–334.

[42] Z.L. Wang, H.B. Liang, M.L. Hong, Q. Su. (2007). Novel red phosphor of Bi^{3+}, Sm^{3+} co-activated NaEu $(MoO_4)_2$. *Optical Materials*. **29**, 896–900.

[43] Wintle, A. G., Geophys. J. R. (1975). Thermal quenching of thermoluminescence in quartz. *American Astronomical Society.* **41**, 107.

[44] Lei B F, Yue S, Zhang Y Z and Liu Y L. (2010). Luminescence Properties of Sr_2SnO_4:Sm^{3+} Afterglow Phosphor. *Chinese Physics Letters*. **27,** 037201

[45] Wu H. Y., Wang Y. H., Hu Y. H., Deng L. Y.. and Xie W. (2009). Controllable optical properties by ratio of Sr/Ca in $Sr_{1.97-x}Ca_xMgSi_2O_7:Eu^{2+},Dy^{3+}$ phosphors. *Journal of Physics D: Applied Physics.* **42,** 125406

[46] Ju Z. H., Zhang S. H., Gao X. P., Tang X. L., and Liu W. S. (2011). Reddish orange long afterglow phosphor $Ca2SnO_4:Sm^{3+}$ prepared by sol–gel method. *Journal of Alloys and Compounds*. **509**, 8082

[47] Ju Z. H., Wei R. P., Zheng J. G., Gao X. P., Zhang S. H. and Liu W. S. (2011). Synthesis and phosphorescence mechanism of a reddish orange emissive long afterglow phosphor Sm^{3+} -doped Ca_2SnO_4. *Applied Physics Letters*. **98,** 121906